Optical side-polished fiber coupler: design and fabrication

Jian Zhang

A Thesis

in

The Department

of

Electrical and Computer Engineering

Presented in Partial Fulfillment of the Requirements
for the Degree of Master of Applied Science
(Electrical and Computer Engineering) at
Concordia University
Montreal, Quebec, Canada

March 2006

Your file Votre référence
ISBN: 0-494-14290-1
Our file Notre référence
ISBN: 0-494-14290-1

ABSTRACT

Optical side-polished fiber coupler: design and fabrication

Jian Zhang

In this thesis, fiber optical ray theory and mode coupling theory are used to analyse the transfer characteristics of fiber optical couplers. For light transmission in telecom optical fibers, the variations of mode numbers and mode field diameter (MFD) are simulated. The transferred and coupled power characteristics of fiber couplers are also simulated. Using the simulation results, some etched couplers, micro optical components, and side-polished fiber couplers are designed and fabricated.

In order to keep the fiber characteristics unchanged, the work is focused on the process of making fiber couplers at room temperature. We used two methods of fabrications, etching fiber and side-polishing fiber to fabricate 2x2 etched fiber couplers and side-polished fiber couplers. Couplers of side-polished fiber are also fabricated. Coupling and structures of the fabricated devices were examined using SEM and microscopic pictures.

Also, in this work, it was tried to fabricate couplers fibers with etched period ditches, however, due to the difficulties of matching the fibers the attempt is failed.

Star couplers and x-couplers in silicon V-grooves, silicon, and in glass substrates are fabricated. In order to couple two polished fibers, a work stage for fiber coupler is designed, which has a coarse horizontal X-Y stage and a vertical Z coarse stage, and a small fine XYZ stage is used to adjust the sample in μm level.

The structures of all the devices were characterized using scanning electron or optical microscopes.

ACKNOWLEDGEMENT

I would like to express my special appreciation to Dr. Mojtaba Kahrizi of Electrical and Computer Engineering Department, for his academic, professional, and devoting instructions during the entire project.

Meanwhile, thanks must be given to Dr. John Zhang of Electrical Engineering Department for his significant technical support; Mr. Shailesh Prasad of Electrical Engineering Department, for his help in lab facilities.

I also would like to thank Mr. Jun Chen and Miss Hong Qu of Electrical and Computer Engineering Department for their professional help and discussion in SEM, and experiments; My friends Mr. Jun Li, Mr. Bowei Zhang, Mr. Li Wei Sun, and Mr. Yu Fan of Electrical and Computer Engineering Department for their valuable support and beneficial discussion in technology; My colleagues in lab Mr Xiaohong Mu, Mr. Zhao Lu, Miss Yaxia Zhang, Mr. ShiQuan Yao, Mr. LiJun Zhang, Mr. Siamak Fouladi and other friends in our semiconductor lab of Computer Engineering Department for their friendly encouragement and discussion.

My wife Lu and my son Leyu deserve an award for their encouragement and understanding during graduate school and during the writing of this thesis. I am grateful for the understanding of my parents and family especially during those times when the research came first.

Finally, I am mournful the loss of Dr. Victor Rossokhaty, who passed away accidentally this summer. When he was a professor of Electrical and computer Engineering Department, his professional advices and valuable technical support gave me lots of enlightenments.

TABLE OF CONTENTS

TABLE OF CONTENTS

CHAPTER PAGE

LIST OF FIGURES

FIGURE PAGE

LIST OF FIGURES

FIGURE PAGE

LIST OF FIGURES

FIGURE PAGE

LIST OF FIGURES

FIGURE PAGE

CHAPTER 1

INTRODUCTION

This chapter includes an overview of major fiber optic coupler technology.

1.1 History

In optical fiber telecommunications F.F Roberts working at The British Telecom Office Research Laboratories identified the idea of optical fiber in 1966. Today, more than 95 percent of the long-distance traffic is transmitted through optical fibers in the world [7].

Advances in fiber optics have permitted the introduction of fiber optics into present applications. These applications are mostly in the telephone long-haul systems, but are growing to include cable television, computer networks, video systems, and data links. All-optical networks are terms of network based on all optical components and devices, in which many cheap and new fiber components are used in the communication networks. For example, there are light fiber amplifiers, wavelength converters, filters, adder/droppers, and fiber couplers. A fiber coupler is one of the most important components in all-optic networks since it is the basic part of many new integrated optical devices, and the biggest challenge remaining for fiber optics is economic issue.

1.2 Fiber Optic Coupler Technology Review

The optical-fiber couplers are particularly important to optical-fiber communications and sensors area. It is frequently a requirement to pass light from one fiber into another fiber or other devices. This process is referred to as "coupling" of light from one fiber to another. For example, in wavelength division multiplexing (WDM), it is required to couple many optical signals at different wavelengths into one fiber, in the hub of a star network, the coupling from a "transmit" fiber into a "receive" fiber, or into the circulating ring of a ring network; for a fiber amplifier or fiber laser, the coupling of pump light into amplifying fiber. Figure 1.1 shows some system architectures that use more complex link designs. In many cases these types of systems require fiber optic components that can redistribute (combine or split) optical signals throughout the system.

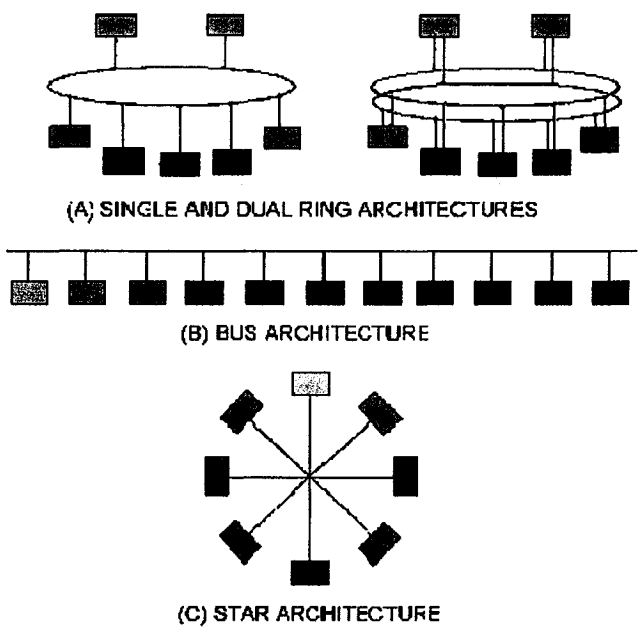

Figure 1.1 Examples of complex system architectures [29].

A fiber optic coupler can also combine the optical signal from two or more fibers into a single fiber. Fiber optic couplers attenuate the signal much more than a connector or a splicer because the input signal is divided among the output ports.

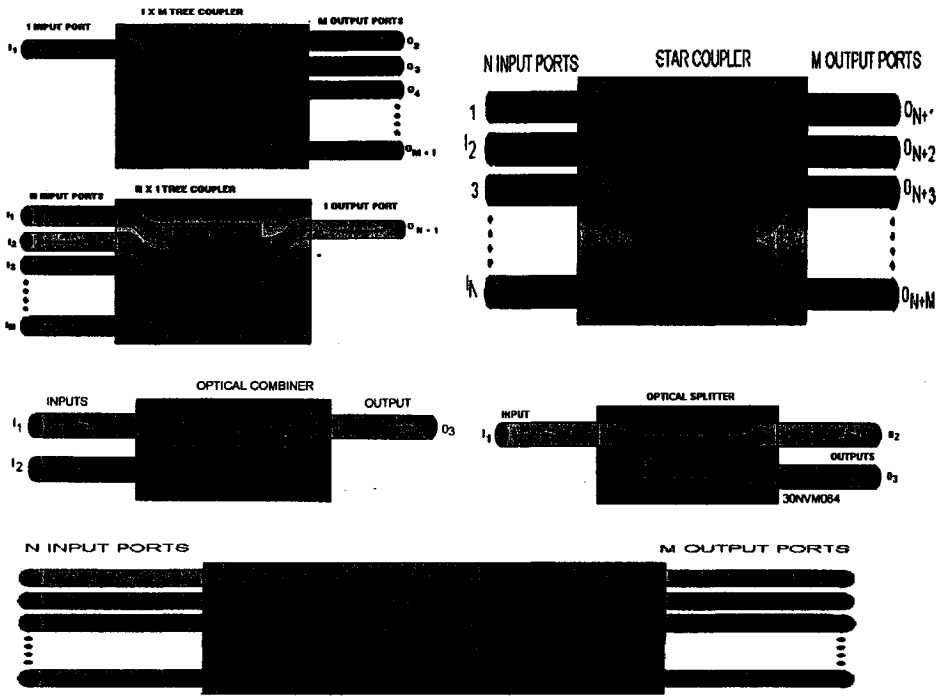

Figure 1.2 coupler examples [29]

Fiber optic couplers can be either active or passive devices. The difference between active and passive couplers is that a passive coupler redistributes the optical signal without optical-to-electrical conversion. Active couplers are electronic devices that split or combine the signal electrically and use fiber optic detectors and sources for input and output [3].

In order to fabricate fiber-optical coupler or other components, it is necessary to modify the fiber structures over distance of several millimeters or centimeters. Such

modifications have been usually achieved by polishing, etching or fusion/tapering of the fibers. In the "polishing" approach, a fiber is bonded to a curved V-groove on a glass or silicon substrate, and polished near the fiber core. In the "etching" approach, the cladding region of the fiber is chemically etched close to the core region in HF or HF-NH_4F solution. In the "fusion/tapering" approach, two or more fibers are securely attached to translation stages and processes of fusion and tapering upon applying suitable heat to fibers with a micro-torch. After Kawasaki made the first fused-fiber coupler, fused-fiber couplers became one of the most popular and important components in commercial market. Among techniques of fabricating couplers, polishing and etching fiber methods are more desirable to researchers since some important fiber characteristics (for example, Bragg Fiber Grating) can be decreased or erased under high temperature like fusion. However, fabrication of fiber couplers with polishing and etching is very challenging.

1.3 Summary of the Work

The thesis is written in six chapters. Chapter 2: background and theory: optical fiber communication theories have been described briefly. It includes optical ray theory and mode theory. Silica material structures and MEMS TMAH etching processes are also introduced. Chapter 3: simulations: it contains simulations for fiber modes and coupler. Chapter 4: designs and fabrication: it describes design and fabrication of maskers, V-grooves, side-polished fibers, and couplers. In Chapter 5, experiments of observing coupling phenomena and their different applications in sensing, couplers, switches and modulators are discussed. The last Chapter (Chapter 6), some conclusions and suggestions for future work are presented.

CHAPTER 2

THEORETICAL BACKGROUND

INTRODUCTION

This chapter introduces two major techniques that are essential in entire research work including the light propagation theories and semiconductor basic knowledge. In light propagation theories part, Ray optics and mode theory are introduced briefly, and mode coupling theory and Mode-excitation theory for optical coupler are also presented. Finally, Silicon etching knowledge is discussed. Upon introductions, a preliminary scheme of fiber optic coupler technology is prototyped, and challenges in making such devices in laboratory are emphasized.

For many years it has been appreciated that the use of optical (light) waves as a carrier wave provides an enormous potential bandwidth. However, the atmosphere is a poor transmission medium for light waves. Optical communication only became a widespread option with the development of low-loss dielectric waveguide. In addition to the potential bandwidth, optical fiber communication offers a number of benefits: Size, weight, flexibility, Electrical isolation, Security, low transmission loss, etc [4].

The primary disadvantage of optical fiber is the technical difficulties associated with reliable and cheap connections, and the development of an optical circuit technology that can match the potential data-rates of the cables. The speed of these circuits, which are electronically controlled, is usually the limiting factor on the bit-rate. The difficulty of

connection and high-cost of associated circuitry result in optical fibers are being used only in very high bit-rate communication. There is considerable current debate as to whether optics will ever completely replace electronic technology [4].

In future, more and more optical components replace electronic components that finally result in an all-optical network. In the latter network, routing and switching functions are also performed optically that result in an end-to-end optical connection.

2.1 History and Type of Optical Fibers

The exact nature of light is not fully understood, although people have been studying the subject for many centuries. In the 1700s and before, experiments seemed to indicate that light was composed of particles. In the early 1800s, a physicist Thomas Young found that light exhibited wave characteristics [5].

Further experiments by other physicists culminated in James Clerk Maxwell collecting the four fundamental equations that completely describe the behavior of the electromagnetic fields. James Maxwell deduced that light was simply a component of the electromagnetic spectrum. This theory seems to firmly establish that light is a wave. Yet, in the early 1900s, the interaction of light with semiconductor materials, called the photoelectric effect, could not be explained with electromagnetic-wave theory.

The advent of quantum physics successfully explained the photoelectric effect in terms of fundamental particles of energy called quanta. Quanta are known as photons when referring to light energy [6].

The concept of light propagation, the transmission of light along an optical fiber, can be described by two theories. According to the first theory, light is described as a simple ray. This theory is the ray theory, or geometrical optics, approach. The advantage of the ray approach is that you get a clearer picture of the propagation of light along a fiber. The ray theory is used to approximate the light acceptance and guiding properties of optical fibers. According to the second theory, light is described as an electromagnetic wave. This theory is the mode theory, or wave representation, approach. The mode theory describes the behavior of light within an optical fiber and some passive optical components.

Refractive index (RI) of a medium is defined as the ratio of the speed of light in free space to its speed in the medium. Optical telecommunication fibers are made usually from silica glasses. The high purity glass is called the host material or substrate. Its bulk reflective index usually defines the refractive index of the fiber cladding. Adding dopant materials to host material forms the fiber core. For example, adding germanium can result in an increase in the refractive index, while adding fluorine reduces it.

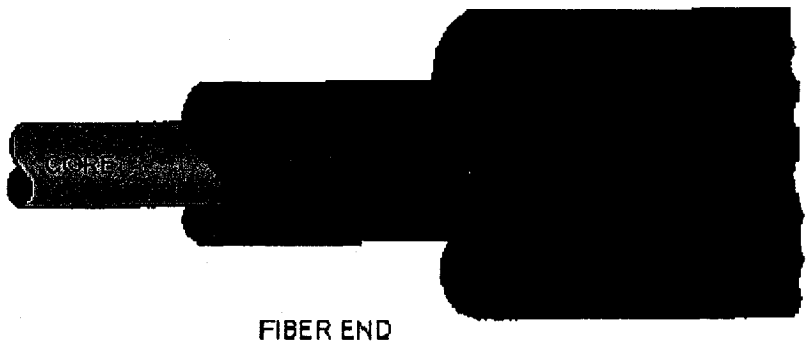

Figure 2.1 Optical fiber structures 1

Assume that n_0 is the refractive index of host material and n_1 is the refractive index of m_1 mole percentage doped material. Then, the refractive index n of m mole percentage doped material can be interpolated as:

$$n^2 = n_0^2 + \frac{m}{m_1}(n_1^2 - n_0^2) \tag{2. 1}$$

The redial distribution of the fiber refractive index is called index profile. That profile determines guiding properties of fiber. In general, the core region has a higher index than the cladding region. However, the index profile can have regions where the index is lower than the cladding value. For example, a dispersion flattened fiber design involves a couple of concentric index regions.

In optical fibers, a useful way of describing a wide range of refractive index radial profiles is through the use of the following relation [7]:

$$n(r) = n_1[1 - 2\Delta(\frac{r}{a})^{\alpha}]^{1/2} \qquad (0 \le r \le a) \tag{2.2}$$

$$= n_2 \qquad (a < r)$$

Where

$$\Delta = \frac{n_1^2 - n_2^2}{2n_1^2} \approx \frac{n_1 - n_2}{n_1} \tag{2.3}$$

and a is the "core" radius. Various profiles can be obtained by varying the parameter α from one to infinity.

The V-number of the fiber can then be written in terms of Δ (Normalized index difference) as

$$V = \frac{2\pi}{\lambda} a n_1 \sqrt{2\Delta} \approx \frac{2\pi}{\lambda} a n_2 \sqrt{2\Delta} \tag{2.4}$$

When V>10, geometrical optics results can be used to describe the propagation effects in optical fibers. For $V \leq 10$, electromagnetic analysis is used to investigate propagation effects in the fibers [8].

Depending on the refraction index of the core whether it is constant or varying, fibers can be classified into two types: Stepped-index and Graded-index fiber. Depending on their properties of transmission, optical fibers are classified into single mode and multimode fibers. As each name implies, the number of modes that propagate along the fiber classifies optical fibers. As previously explained, the structure of the fiber can permit or restrict modes from propagating in a fiber. The basic structural difference is the core size.

Typically, single mode fiber has a much smaller core radius and smaller Δ than multimode fibers. If the wavelength λ of the source is reduced sufficiently, a single mode fiber will become multimode as V will exceed 2.405, and high modes will also contribute to propagation. The cut-off wavelength λ above which the fiber become single mode is given by [8]

$$V_{cut-off} = \frac{2\pi}{\lambda_c} a n_1 \sqrt{2\Delta} \approx \frac{2\pi}{\lambda_c} a n_2 \sqrt{2\Delta} = 2.405 \tag{2.5}$$

The number of modes will rise rapidly when the V-number increases above 2.405. For step-index fiber, the approximate number of modes is given by

$$M \approx \frac{V^2}{2} \tag{2.6}$$

For a planar dielectric waveguide, the approximate number of modes is given by

$$M = \text{int}\left(\frac{2V}{\pi}\right) + 1 \tag{2.7}$$

There are 3 kinds of fibers according to their RI profiles: stepped-index multimode fiber (typical cladding diameter is 125 to 400μm, and core diameter 50 to 200 μm), graded-index multimode fiber (typical cladding diameter is 125 to 140μm, and core diameter 50 to 100 μm), and single -mode fiber (typical cladding diameter is 125μm, and core diameter 8 to 12 μm). Figure 2.2 -2.4 show various types of fibers. PANDA fiber and elliptical-cladding single-mode fiber belong to single mode fiber.

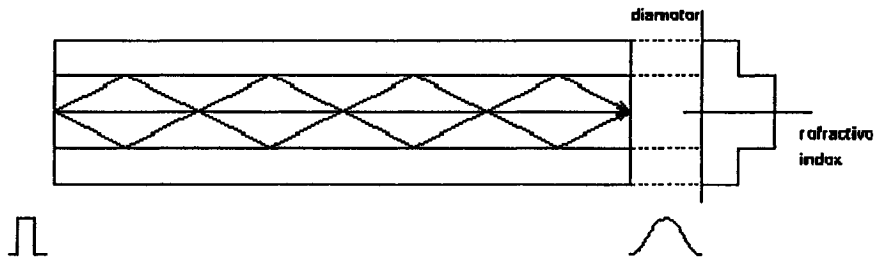

Figure 2.2:Stepped-index fibers

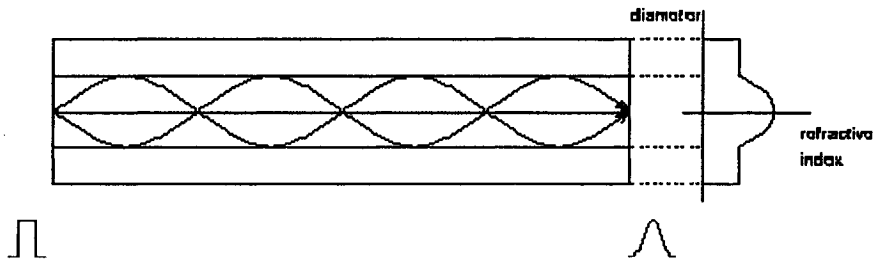

Figure 2.3:Graded-index fiber

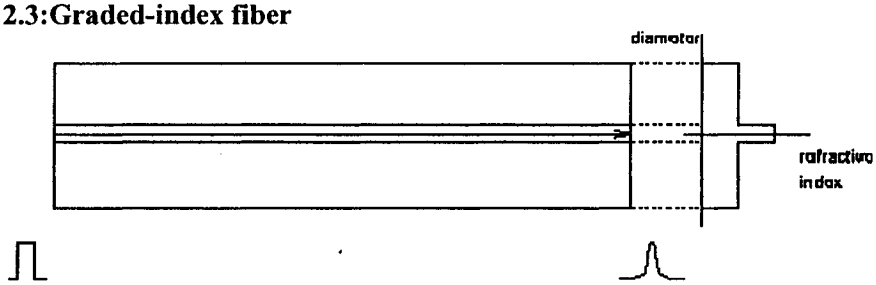

Figure 2.4: Mono-mode fiber

2.2 Ray Theory

Two types of rays can propagate along an optical fiber. The first type is called meridional rays. Meridional rays are rays that pass through the axis of the optical fiber. Meridional rays are used to illustrate the basic transmission properties of optical fibers

(Figure 2.5). The second type is called skew rays. Skew rays are rays that travel through an optical fiber without passing through its axis [8].

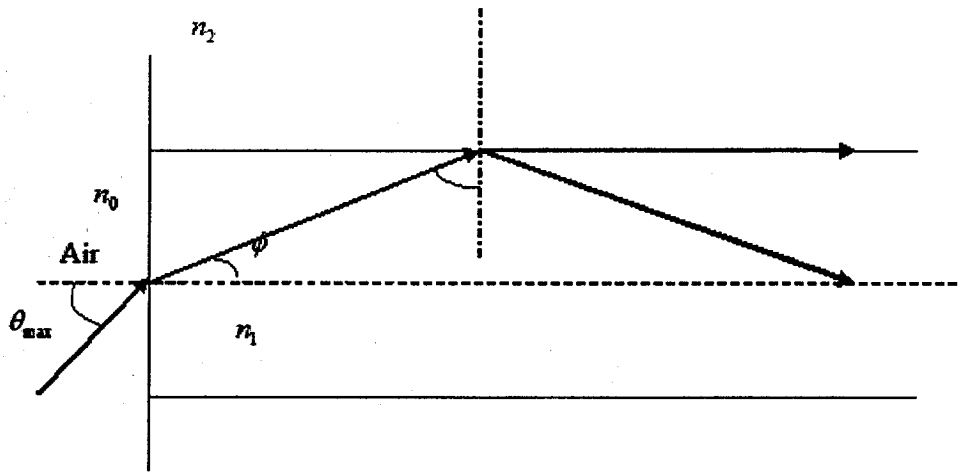

Figure 2.5 Meridional ray propagation in a step index fiber

According to SNELL's law, when light wave transfers in fiber waveguide, the condition for total internal reflection (TIR) at core cladding is given by $n_1 \sin(\pi/2 - \phi) \geq n_2$. Since the angle ϕ is related with the incident angle θ by $n_0 \sin\theta = n_1 \sin\phi \leq \sqrt{n_1^2 - n_2^2}$, where n_0=1 (air), we obtain the critical condition for the total internal reflection as

$$\theta \leq \sin^{-1}\sqrt{n_1^2 - n_2^2} \equiv \theta_{max} \tag{2.8}$$

The refractive index difference between core and cladding is of the order of 0.01, so θ_{max} can be approximated. θ_{max} (Maximum entrance angle) denotes the maximum light

acceptance angle of the fiber waveguide. The above equation also defines the numerical aperture (NA) of a step index fiber (SI) for meridional rays.

$$NA = n_0 \sin \theta_{max} = \sqrt{n_1^2 - n_2^2} = n_1 \sqrt{2\Delta} \tag{2.9}$$

It is a dimensionless quantity, which is normally less than unity and ranges from 0.14 to 0.50. Typically NA of telecommunication fibers is 0.1 to 0.2, which implies an acceptance angle of 5.7^o to11.5^o.

2.3 Mode Theory

A set of guided electromagnetic waves is called the modes of an optical fiber. Mode theory is used to describe the types of plane waves able to propagate along an optical fiber. In mode theory, we have to solve the *Maxwell's equations,* which subjected to the cylindrical boundary conditions of the fiber. It is too complex to perform mathematical calculations in the sector. Therefore, a briefly introduction is presented.

When we extend the plane dielectric slab wavelength theory to circular optical fibers, electromagnetic waves are considering in a cylindrical coordinate system (r, ϕ, z). The wave equation from the Maxwell's equations in cylindrical coordinate is given by [10]

$$\frac{\delta^2 E_z}{\delta r^2} + \frac{1}{r}\frac{\delta E_z}{\delta r} + \frac{1}{r^2}\frac{\delta^2 E_z}{\delta \phi^2} + \frac{\delta^2 E_z}{\delta z^2} - \frac{n^2}{c_0^2}\frac{\delta^2 E_z}{\delta t^2} = 0 \tag{2.10}$$

and

$$\frac{\delta^2 H_z}{\delta r^2}+\frac{1}{r}\frac{\delta H_z}{\delta r}+\frac{1}{r^2}\frac{\delta^2 H_z}{\delta \phi^2}+\frac{\delta^2 H_z}{\delta z^2}-\frac{n^2}{c_0^2}\frac{\delta^2 H_z}{\delta t^2}=0 \qquad (2.11)$$

Where E_z and H_z are z-components of electric and magnetic fields respectively. c_0 is the velocity of light in vacuum, and n is the refractive index of medium. Since the electromagnetic waves are to propagate along the z-axis, these will have a functional dependence of the form.

$$E_z(r,\phi,z)=E_z(r,\phi)\exp[-j(\omega t-\beta z)] \qquad (2.12)$$

And

$$H_z(r,\phi,z)=H_z(r,\phi)\exp[-j(\omega t-\beta z)] \qquad (2.13)$$

In general, Boundary conditions of the electromagnetic field components require the coupling of E_z and H_z. The cylindrical waveguide is bounded in two dimensions rather than one.

2.3.1 Fiber Propagation Modes

The mode theory, along with the ray theory, is used to describe the propagation of light along an optical fiber. The mode theory is used to describe the properties of light that ray theory is unable to explain. The mode theory uses electromagnetic wave behavior to describe the propagation of light along a fiber [9].

A set of guided electromagnetic waves is called the modes of an optical fiber. Maxwell's equations describe electromagnetic waves or modes as having two

components. The two components are the electric field, E (x, y, z), and the magnetic field, H(x, y, z). The electric field, E, and the magnetic field, H, are at right angles to each other. Modes traveling in an optical fiber are said to be transverse. The transverse modes, shown in figure 2.6, propagate along the axis of the fiber. The mode field patterns shown in figure 2.6 are said to be transverse electric (TE) modes. In TE modes, the electric field is perpendicular to the direction of propagation.

The magnetic field is in the direction of propagation. Another type of transverse mode is the transverse magnetic (TM) mode. TM modes are opposite to TE modes. In TM modes, the magnetic field is perpendicular to the direction of propagation. The electric field is in the direction of propagation. Figure 2-6 [8] shows only TE modes.

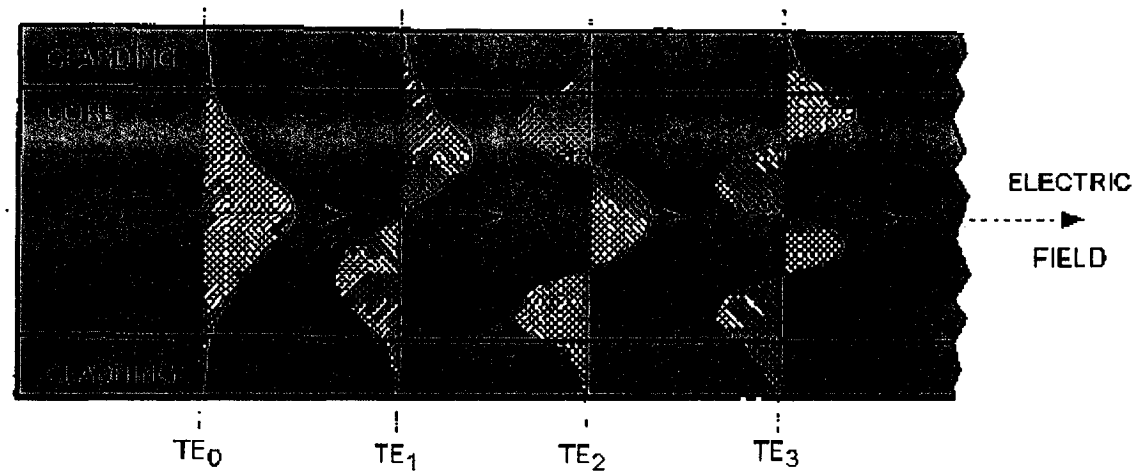

Figure 2.6 Transverse electric (TE) mode field patterns [8]

The TE mode field patterns shown in figure 2-6 indicate the order of each mode. The order of each mode is indicated by the number of field maxima within the core of the

fiber. For example, TE_0 has one-field maxima. The electric field is a maximum at the center of the waveguide and decays toward the core-cladding boundary. TE_0 is considered the fundamental mode or the lowest order standing wave. As the number of field maxima increases, the order of the mode becomes higher. Generally, modes with more than a few (5-10) field maxima are referred to as high-order modes. The order of the mode is also determined by the angle that the wave front makes with the axis of the fiber. Figure 2.7 illustrates light rays as they travel down the fiber. These light rays indicate the direction of the wave fronts. High-order modes cross the axis of the fiber at steeper angles. Low-order and high-order modes are shown in figure 2.7[8].

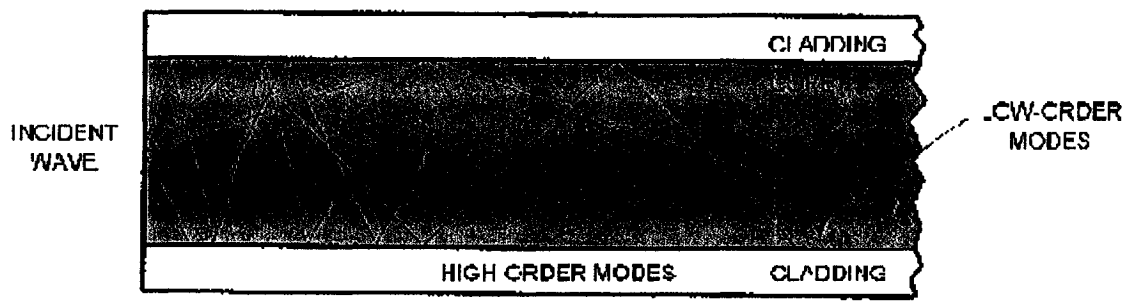

Figure 2.7 Low-order and high-order modes

In general, the cylindrical waveguide is bounded in two dimensions rather than one. Thus, two integers, l and m, are necessary to specify the modes, in contrast to single integer m required for the planar guide. Thus in a cylindrical waveguide, TE_{lm} and TM_{lm} modes will exist. These modes correspond to meridional rays traveling within a fiber. In Optical fibers the core-cladding boundary conditions lead to a coupling between the electric and magnetic field components. This gives rise to hybrid HE and EH modes. In weak guidance such as in optical fibers ($\Delta<<1$), HE-EH mode pairs occur and they have almost identical propagation constant. In order to simplify the analysis of mode

propagation, The superposition of these modes characterized by a common propagation constant corresponds to a particular linearly polarized (LP) mode regardless of their HE, EH, TE or TM field configurations. It may be observed from the field configurations of modes that the field strength in the transverse direction is identical for the modes that belong to the same LP mode. The LP (l, m) modes are designated by two numbers: l – azimuthal number and m – orbital number, where l=0, 1, 2 ... and m=1, 2,... The fundamental mode of fiber is LP (0, 1) [11].

There are some relationships between HE, EH, TE and TM modes and the LP_{lm} modes in table 2.1[4].

LP mode	Traditional Mode
LP_{01}	HE_{11}
LP_{11}	$HE_{21}TE_{01}TM_{01}$

Table 2.1 Composition of the lower-order LP mode

Notice that the modes are not confined to the core of the fiber. The modes extend partially into the cladding material. Low-order modes penetrate the cladding only slightly. In low-order modes, the electric and magnetic fields are concentrated near the center of the fiber. However, high-order modes penetrate further into the cladding material. In high-order modes, the electrical and magnetic fields are distributed more toward the outer edges of the fiber.

This penetration of low-order and high-order modes into the cladding region indicates that some portion is refracted out of the core. The refracted modes may become trapped in the cladding due to the dimension of the cladding region. The modes trapped in the cladding region are called cladding modes. As the core and the cladding modes travel along the fiber, mode coupling occurs. Mode coupling is the exchange of power between two modes. Mode coupling to the cladding results in the loss of power from the core modes.

One definition of MFD was introduced from planar waveguide as well as it is will be used in fiber waveguide. It based on the fact that the field distribution is harmonic within the core, whereas from the boundary into the cladding. The field is due to the evanescent wave and decays exponentially.

$$E_{cladding}(y') = E_{cladding}(0)\exp(-\alpha_{cladding} y') \tag{2.14}$$

$$\alpha_{cladding} \approx \frac{V}{a} \tag{2.15}$$

where a is the radius of the fiber core. The field in cladding decays by as factor of e^{-1} when $y' = \delta = 1/\alpha_{cladding} = a/V$. The extent of field in the cladding is about δ. The total extent of the field across the whole guide is therefore $2a + 2\delta$, which is called the mode field diameter (MFD) and denoted by $2\omega_0$

$$2\omega_0 = 2a + 2\delta \approx 2a + 2\frac{a}{V} = 2a\frac{(V+1)}{V} \tag{2.16}$$

We note that as V increases, MFD becomes the same as the core thickness, 2a. In single mode case, when V reduce to be fewer than 2.405, and MFD is considerably larger than 2a, where a is the radius of the fiber core.

2.3.2 Mode coupling between two parallel channel waveguides

Coupled Mode Theory is a method to analyze the light propagation in perturbed or weakly coupled waveguides. The basic idea of the Coupled Mode Theory method is that the modes of the unperturbed or uncoupled structures are defined and solved. The theory assumes that the field of the coupled structures may be sufficiently represented by a linear superposition of the modes of the unperturbed structures. In many practical cases, this assumption is valid and does give an insightful and often accurate mathematical description of electromagnetic wave propagation. The Coupled Mode Theory is most useful in the analysis of the interaction between several near resonance-guided modes, and it has been widely used and proven to be one of the most productive and efficient methods for the analysis of waveguide devices [4].

It is easy to consider two fundamental modes in both waveguides A and B. The fundamental modes, A and B, are separated each other before they propagate along with the guide, and they propagate independently with field patterns $E_A(x,y)$ and $E_B(x,y)$, also with propagation constants β_A and β_B. Here subscripts A and B refer to guiding modes A and B. While the waveguides are brought into proximity, the overlay of evanescent field will cause interferential coupling. As a result the power of the guided mode will be coupled from one guide to the adjacent guide.

In such a composite structure, the wave can be represented by the exact solutions of the guided modes from Maxwell's equations, or wave equations. Solving the wave equations is not easy for such a composite waveguide structure, and the closed form solution is often not available. An easy way to get the solution for a weakly perturbed system is from the coupled-mode analysis. The electric field is represented by a linear combination of the unperturbed guided modes with varying amplitudes. Variation of the amplitudes with distance indicates the transfer of energy between the unperturbed modes. The modes of propagation of the individual waveguides are $E_A(x,y)\exp[i(\omega t-\beta_A z)]$ and $E_B(x,y)\exp[i(\omega t-\beta_B z)]$. Assuming that waves propagate only in the forward direction, the electric field in coupler-guide structure can be approximated by a linear combination of two independent original modes, when the two waveguides are not too close to each other [13] [14].

$$E(x,y,z,t)=A(z)E_A(x,y)\exp[i(\omega t-\beta_A z)]+B(z)E_B(x,y)\exp[i(\omega t-\beta_B z)] \qquad (2.17)$$

The refractive index in this structure is presented as

$$n^2(x,y)=n_s^2+\Delta n_A^2(x,y)+\Delta n_B^2(x,y) \qquad (2.18)$$

where $\Delta n_A^2(x,y)$ and $\Delta n_B^2(x,y)$ represents the presence of waveguides A and B and both vanish except at the cores of waveguides A and B, as show in figure 2.8 [16].

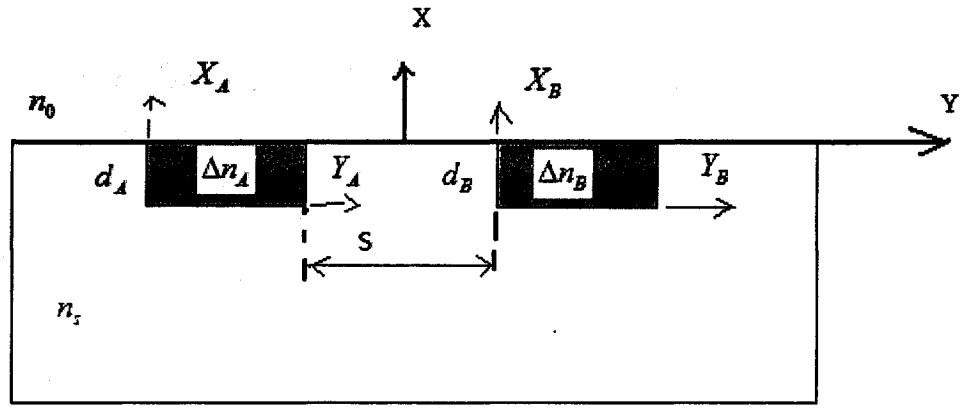

Figure 2.8: Coupled dissimilar channel waveguide geometry

After complex mathematical calculations were performed, K_{ij} was given as [16]:

$$K_{ij} = \frac{K_0^2}{2\beta_i} \frac{\int\int E_i^*(x,y).\Delta n_i^2(x,y)E_j(x,y)dxdy}{\int_{-\infty}^{\infty}\int_{-\infty}^{\infty} E_i^2(x,y)dxdy} \qquad (2.19)$$

where i,j=A,B, k_{AA} and k_{BB} represent the self-coupling of the guides, while k_{AB} and k_{BA} describe the mutual coupling between the guides.

2.3.3 Mode-excitation Theory

In 1986, "Mode Excitation Theory" was proposed by Mao, Fang and Li in their paper [17]. They divided optical couplers into two groups according to coupling mechanism: weakly coupling and strongly coupling devices. The first group is characterized by the fact that the modes become coupled through their evanescent fields, and its coupling mechanism can be analyzed by using the coupled mode theory

[17][18][19]. In the second group, it is characterized by the fact that the coupling zone of such a coupler is regarded as a new single waveguide, the beat phenomenon between modes result in the exchange of energy [21]. They indicated side-polished fiber couplers are considered as strong coupling couplers in the second group [17]. Such a coupler consists of two parallel-spliced fibers with their cores touching each other; therefore, it cannot be neglected anymore as the core of the coupling zone still plays most important role in guidance of light wave[17].

The key points of the mode excitation theory are as follows: first of all, the coupling zone is considered as a unique waveguide, with its start plane A (Figure 2.8) as a discontinuity interface of the waveguide, the excitation coefficients of the propagation modes in the coupling zone excited by the modes in the input branch waveguide can be found according to the boundary condition (continuity of tangential field). Second, these propagation modes have different phase shifts when they arrive at the end plane B of the coupling zone (Figure 2.9) because they travel with different velocities through the same coupling length L.

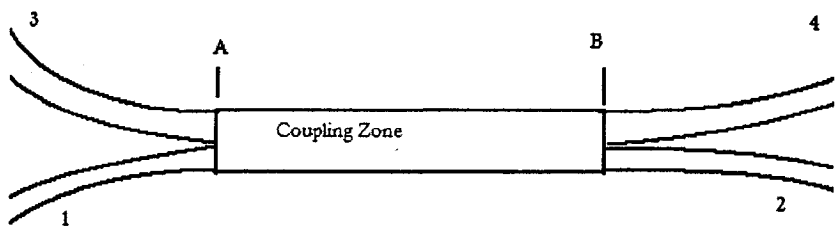

Figure 2.9: Top view of a directional coupler with strong coupling

Third, at this interface B, they excite back all the propagation modes in the branch waveguides 2 and 4 with their own phases, and each mode field in the branch waveguide can be obtained by the superposition of all components excited by the propagation modes in the coupling zone. Fourth, the square of the mode field amplitude corresponds to the mode power, and the sum of all the mode powers gives the total output power of the port, from which the theoretical coupling amount and the insertion loss can be estimated. The cutting depth and the coupling length can be measured and monitored by an especially effective photoelectrical technique as the core has been cut down and polished partially. Using this technique to control the coupling length, several couplers with various coupling amounts had been made by them.

2.4 Transfer Matrix Method for 2X2 coupler

Several useful properties of many optical devices can be obtained by considering the simple case of a 2X2 coupler. Whatever they are fused fibers couplers, planar waveguides or side-polished fiber couplers, much of the input field propagations outside the original fiber core, and this decoupled field can be re-coupled into the other fiber [4].

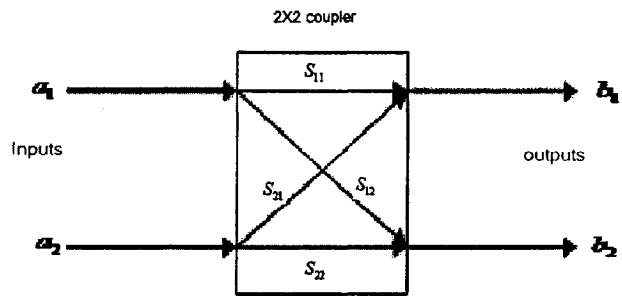

Figure 2.10: 2x2 coupler with relevant parameters of the scattering matrix [4]

These couplers can be analyzed in terms of the scattering matrix S. It defines the relationship between the two input field strengths a_1 and a_2 and the two output field strengths b_1 and b_2 [4]

$$\begin{bmatrix} b_1 \\ b_2 \end{bmatrix} = \begin{pmatrix} s_{11} & s_{12} \\ s_{21} & s_{22} \end{pmatrix} \begin{bmatrix} a_1 \\ a_2 \end{bmatrix} \tag{2.20}$$

Where the S_{ij} represents the coupling coefficient from input port j to out port I. assuming $S_{12} = S_{21}$ and lossless device in energy conservation

In practice, passive devices always have some associated excess loss β, which is defined as the fraction of total input power that appears as the total output power

$$\beta = -10\log_{10}\left[\frac{\sum P_{out}}{\sum P_{input}}\right] \tag{2.21}$$

Normally, the β value is ranging from 0.1dB to 0.5 dB. It includes radiation, scattering, absorption losses and coupling loss to isolated port. The directional isolation is the ratio of the backscattered power received at the second input port to that of the input power. The isolation in decibels ranges about 30 dB to 50dB. In specifying the performance of optical coupler, one usually indicates the percentage division of optical power between the output ports by means of the splitting ratio or coupling ratio.

$$\text{splitting ratio} = \left(\frac{P_{b2}}{P_{b1}+P_{b2}}\right)\bullet 100\% \tag{2.22}$$

By adjusting the parameters so that power is divided evenly, each create a 3-dB coupler. A coupler could also be made in which almost all the optical power at 1550nm goes to one port and almost all the energy around 1300nm goes to the other port.

The insertion loss refers to the loss for a particular port-to-port path. For example, for the path from input port I to out port j, we have, in decibels,

$$\text{insertion ratio} = 10\log\left(\frac{P_i}{P_j}\right) \tag{2.23}$$

Another performance parameter is crosstalk (Isolation, Directivity), which measures the degree of isolation between the input at one port and the optical power scattered or reflected back into the other input port. In figure 2.10, it is a measure of optical power level a2:

$$\text{Crosstalk} = 10\log\left(\frac{P_{a2}}{P_{a1}}\right) \tag{2.24}$$

2.5 Etching Background

The Silicon etching processes can be grouped into dry etching and wet etching. Both of them can be divided into isotropic or anisotropic etching. For example, HF etching S_iO_2 on Si masked by photo resist is Wet isotropic etching, and KOH and TMAH

etching Si seeking <111> planes is Wet anisotropic etching. Plasma-assisted etching is an example of Dry anisotropic etching.

Isotropic etching has same etch rate in all directions, lateral etch rate is about the same as vertical etch rate, and etch rate does not depend upon the orientation of the mask edge; however, anisotropic etching has etching rate depending on orientation to crystalline planes. Lateral etching rate can be much larger or smaller than vertical etch rate. Orientation of mask edge to crystalline axes, and orientation of mask edge and the details of the mask pattern determine the final etched shape. Therefore, anisotropic etching can be very useful for making complex shapes .

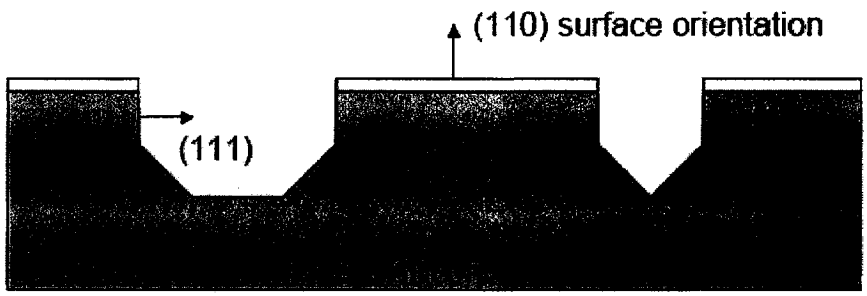

Figure 2.11: Anisotropic etching 1 of Silicon [27]

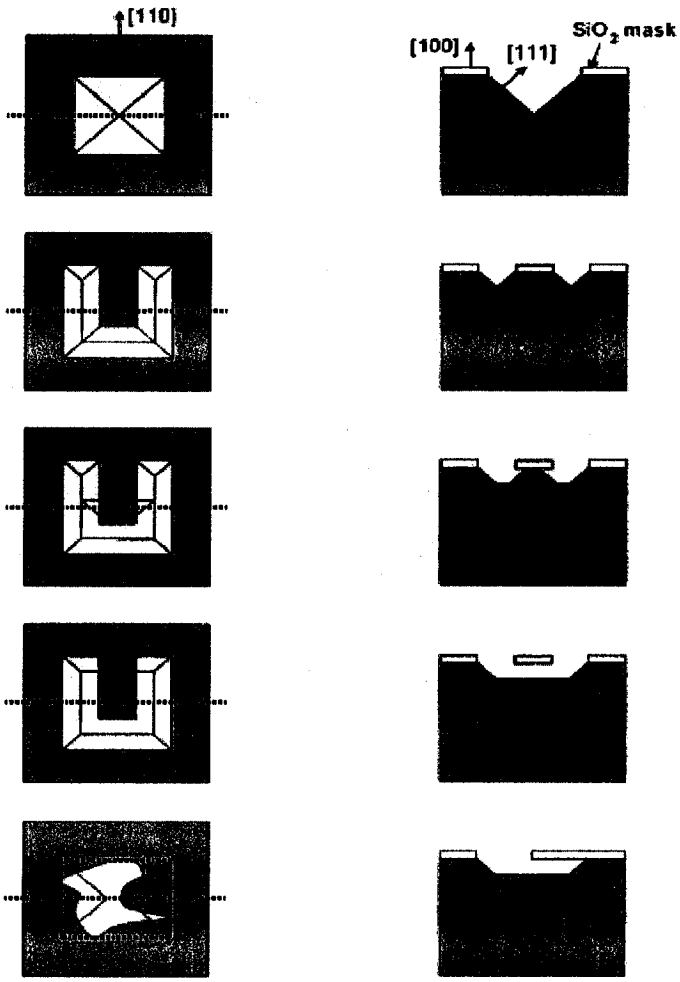

Figure 2.12: Anisotropic etching 2 of Silicon [27]

In this work, we used HF and TMAH wet etching. There are three steps in Wet etching: reactant transport to surface, surface reaction, and reaction product removal from surface.

A buffered HF is used to etch S_iO_2 with photo resist mask, and KOH or TMAH are used to etch S_i with S_iO_2 mask. Similar to KOH etching, TMAH is commonly used for fast removal and silicon micromachining .They have much different etching rate in Si different planes, for example, 22% TMAH in H_20 at 90 degrees temperature <110> plane

etching rate is about 100 times then the one for plane <111>[23]. Therefore, TMAH solution selects S_i planes and stops etching at plane <111>, and they are used widely in MEMS research and industry.

There are two major Silicon wafers, which are widely used for etching V-grooves. One is <100>, and the other is <110>. Both of them should be carefully organized and designed. Basically, In contrast to<100> Silicon wafer, where the four sidewalls of etched always intersect the surface at 54.74°, a <110> wafer yields different geometrical results at anisotropical etching. There are six <111> planes that can be exposed and intersect with the <110> surface, and therefore the top view of an etched cavity is hexagonal with three pairs of parallel sides.

For <110> wafer, it is better that getting a small piece of wafer and etching a litter cave to observe the plane <111> direction. Then, design the position and the direction for your masks since V-grooves (35.26°) and trenches (with vertical sidewalls) that can be created in <110> wafer (figure 2.13 [25]) [26].

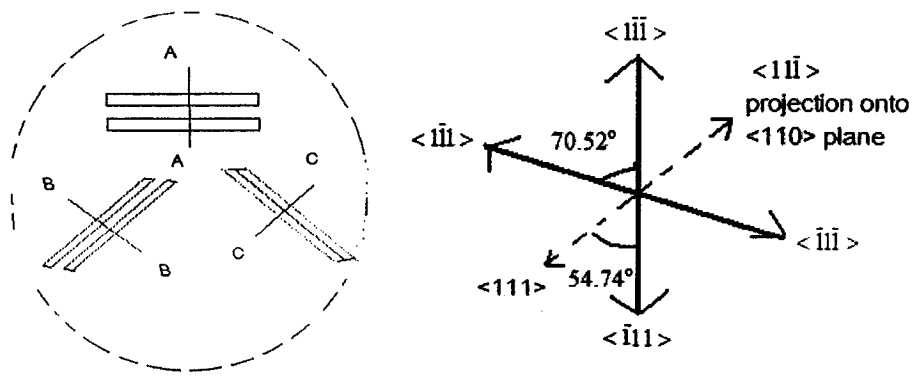

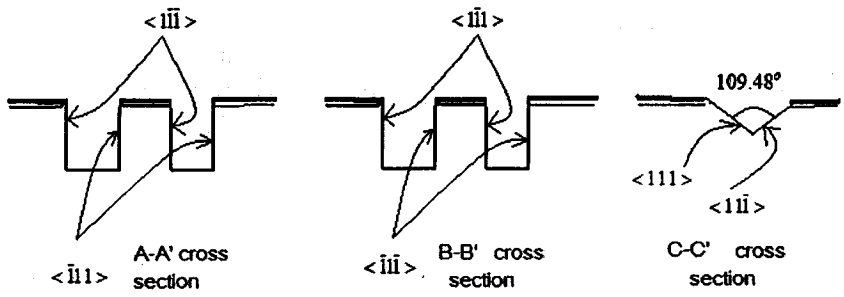

Figure 2.13: Parallel trenches with vertical sidewalls and shallow V-grooves

CHAPTER 3

SIMULATION

INTRODUCTION

In this Chapter, simulations of mode propagation and of coupling between the two waveguides as well as between fibers are presented. For this purpose, an Optiwave simulation tools called Optiwave Optical Fiber design and Optical Grating is used. As it was introduced in previous chapter, when light goes through coupling area, the light can be coupled into a second fiber if the two fiber cores are close to each other. The coupled power depends on wavelength, diameters and reflection indexes of fiber core and cladding, the distance between the two fiber cores, the coupling length of the coupling section and etc. In detail, when the coupling length is fixed, the coupling power is varied with the distance between the two cores, and if the distance of two cores is fixed, the coupling length will change periodically the coupling power.

3.1 Fiber Propagation Modes and mode field diameter

An optical fiber is a dielectric waveguide that operates at optical frequencies. This fiber waveguide is normally cylindrical in form. It confines electromagnetic energy in the form of light to within the surfaces and guides. The transmission properties of an optical waveguide are dictated by its structural characteristics, which have a major effect in determining how an optical signal is affected as it propagates along the fiber. The structure basically establishes the information-carrying capacity of the fiber.

The propagation of light along a waveguide can be described in terms of a set of guided electromagnetic waves called the modes of the waveguide. These guided modes are referred to as bound or trapped modes of the waveguide. Each guided mode is a pattern of electric and magnetic field distributions that is repeated along the fiber at equal intervals. Only a certain discrete number of modes are capable of propagating along the guide. These modes are those electromagnetic waves that satisfy the homogeneous wave equation in the fiber and the boundary condition at the waveguide surface.

It was presented in Chapter 2 section 2.4; a set of guided electromagnetic waves are called the modes of an optical fiber. Maxwell's equations describe electromagnetic waves or modes as having two components, the electric field, E and the magnetic field, H. There is a small difference between core and cladding refractive index in weakly guiding fibers. In weak guidance, like telecommunication fibers, Linearly Polarized (LP) Fiber modes are familiar for us. The LP (l, m) modes are designated by two numbers: l – azimuthal number and m – orbital number, where l=0, 1, 2, ... and m=1, 2, ... The fundamental mode of fiber is LP (0,1) (see modes in figure 3.1).

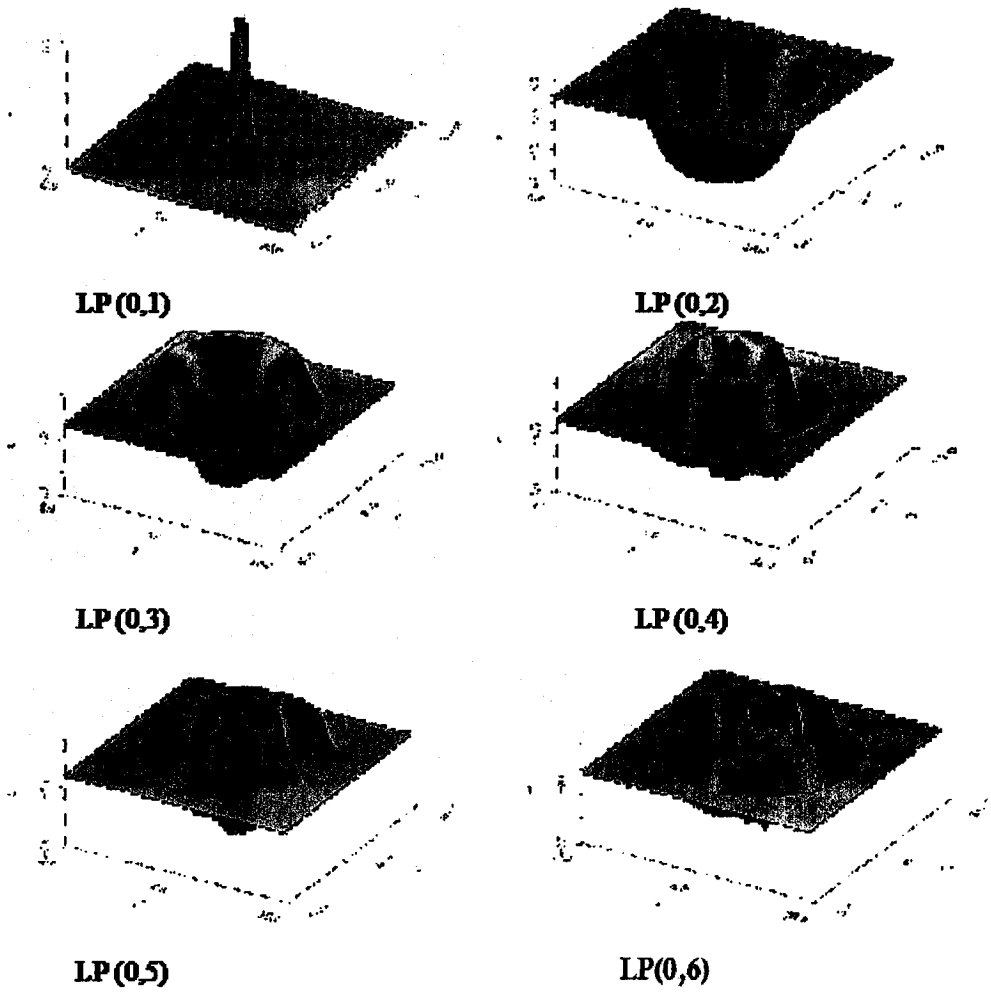

Figure 3.1 3-dimensional LP modes figures

a) Multimode in fiber

The most widely used structure of optical waveguide configurations is the single solid dielectric cylinder of radius a and index of refraction n_1. This cylinder is known as the core of the fiber. The core is surrounded by a solid dielectric cladding which has a refractive index n_2 that is less than n_1.

In order to compare each other in simulation, the cladding diameter of an optical fiber was kept the same size as 125 μm. The light wavelength was set at 1550nm. While

the size of the optical fiber core varies, the propagated modes of the optical fiber are changed in simulations.

There are two modes LP (0,1) and LP (1,1) in light propagation modes when core diameter is set at 12.5μm. In this case, the optical fiber is working in multimode, and the fiber is called multimode fiber. Those two modes, which are defined as patterns of electric and magnetic field distributions along with the fiber, are shown in figure 3.2, 3.3 and 3.4 with normalization intensity and locations in the optical fiber,

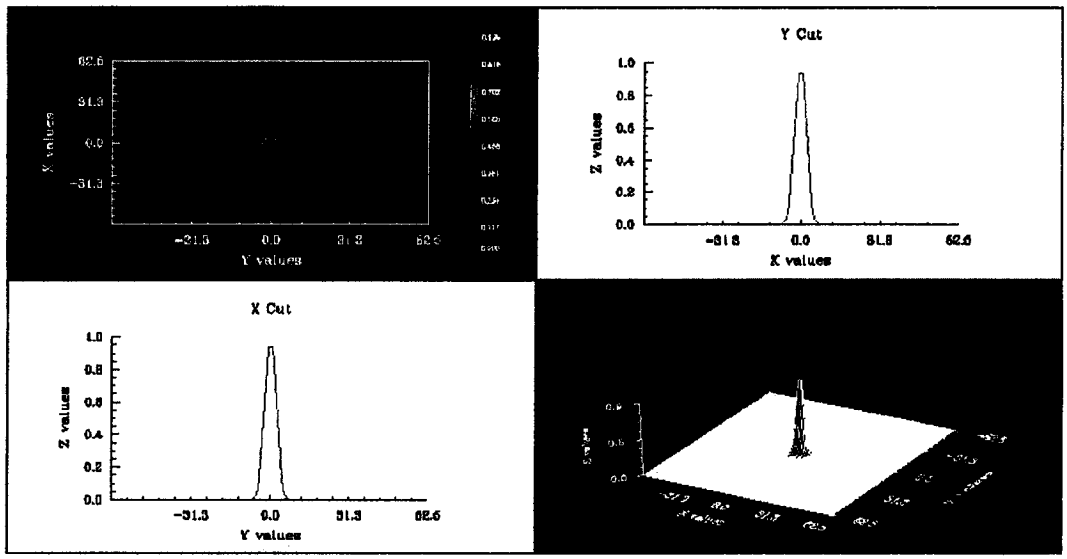

Figure 3.2 LP (0,1) Mode maps

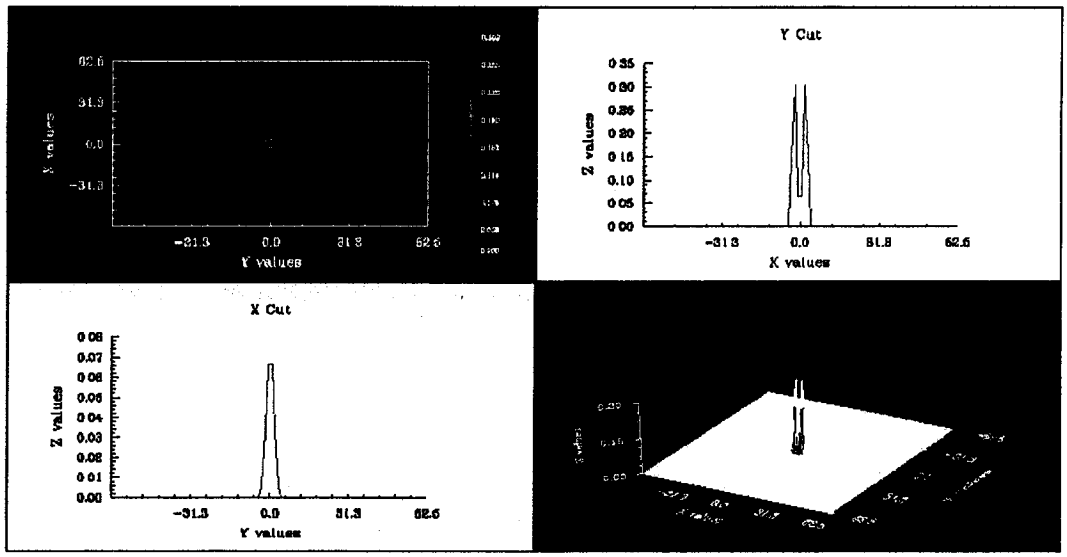

Figure 3.3 LP (1,1) Mode maps

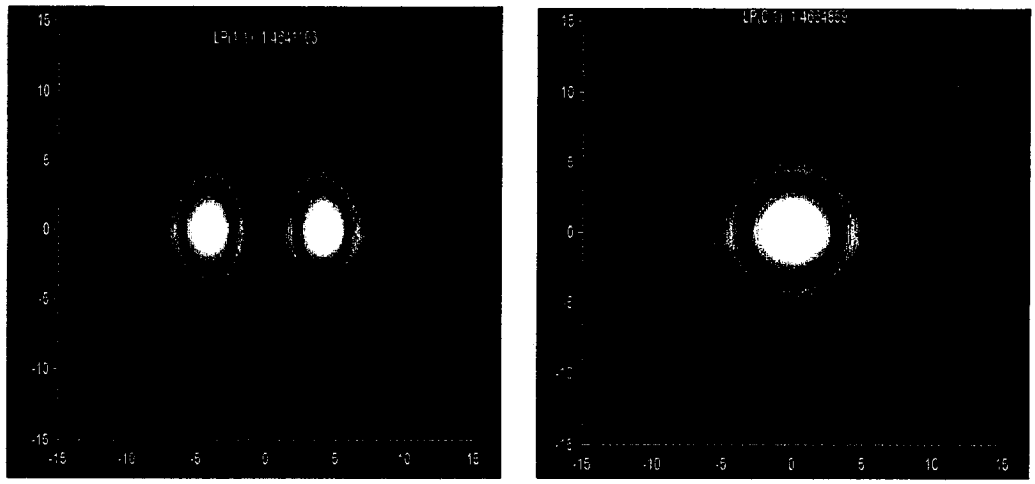

Figure 3.4 LP01 and LP11 modes

b) Single mode in fiber

The same size of cladding fiber was used again. This time, a smaller size (8.3 μm) of core diameter is defined. It is described in chapter 2 that LP (1,1) mode couldn't propagate along with the fiber since V-number is fewer than 2.405. This is confirmed in simulation results, and LP (0,1) mode always stay in the optical fiber propagations. The size of the LP (0,1) mode pattern was shown in Figure 3.5. The diameter of the pattern is about 15 μm.

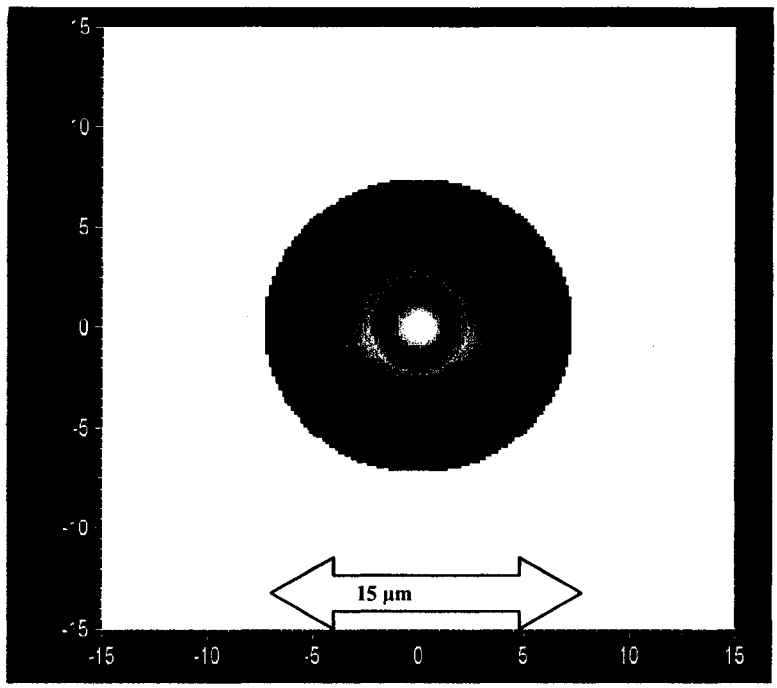

Figure 3.5 LP (01) mode (fiber core diameter 8.3 μm)

c) Single mode MFD varies with fiber core size in fiber

While the size of optical fiber core diameter was set to 4 μm, LP(0,1) mode is the only mode which could propagate in the optical fiber, but the size of LP (0,1) mode pattern become wider (around 36 μm in diameter) than the one of 8.3 μm optical fiber (figure 3.6).

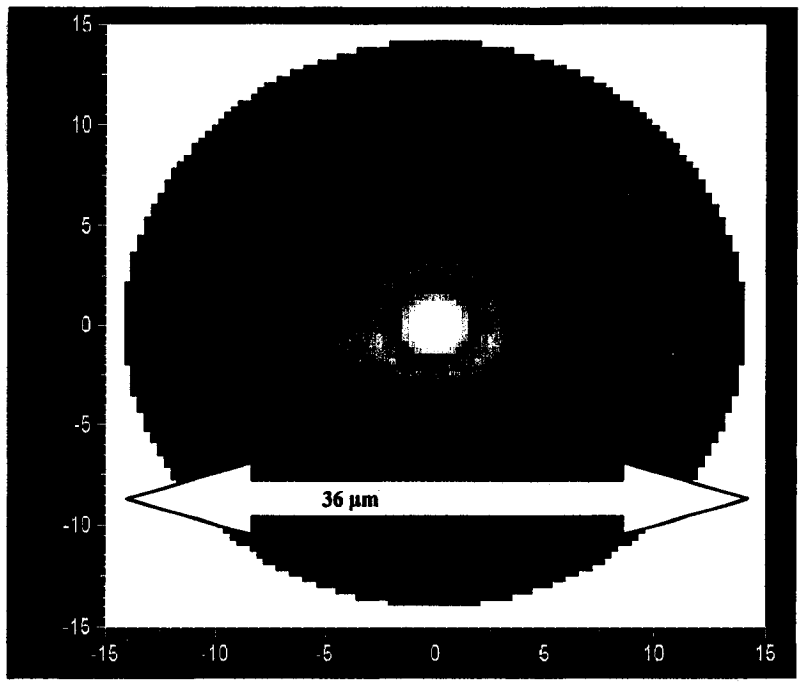

Figure 3.6 LP01 mode (core diameter 4 µm)

From these simulations, we know 4µm core diameter fiber has much bigger mode field diameter in LP (0,1) mode than the one of 8.3µm diameter core fiber. Since smaller core SM fiber has wider diameter of LP (0,1) mode pattern, it is easier to couple the light into other fibers than that of using the fiber with bigger core diameter. From equation 2.16 in chapter two, we also get the same results. In single mode case, when V reduce to be fewer than 2.405, LP (0,1) MFD is considerably larger than 2a, where a is the radius of the fiber core (see Figure 3.5). As the radius of the fiber core is reduced to 4 µm, MFD become 4 times bigger than fiber core diameter, 2a.

d) Single mode MFD vs frequency of light and size of cladding

In this step of simulation, we keep core size same as we did in simulation c (4 μm diameter) and cladding diameter 125 μm. It shows that MFD and its effective area increase while the wavelength increases (Figure 3.7).

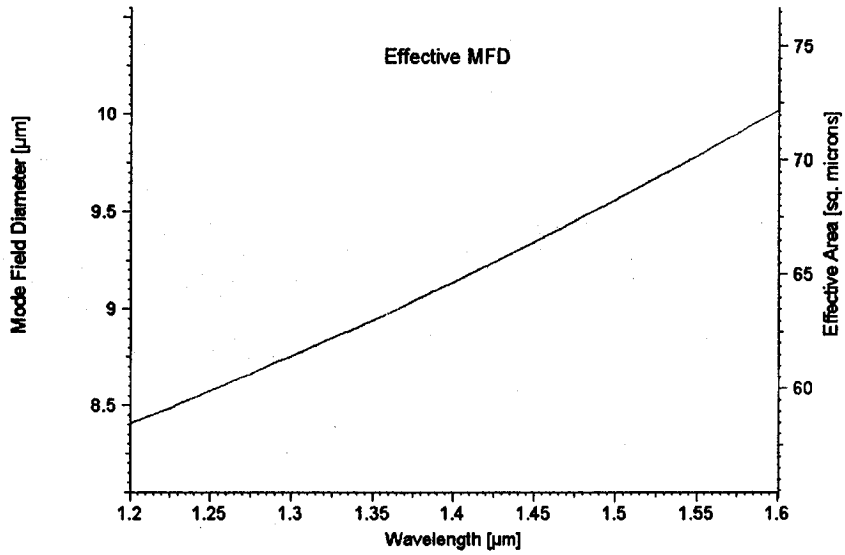

Figure 3.7 Effictive MFD wavelength function1

As we change setting of cladding diameter to 30.5 μm, a result (see figure 3.18) was gotten from simulation. It shows LP(0,1) mode MFD increases while cladding diameter decreases.

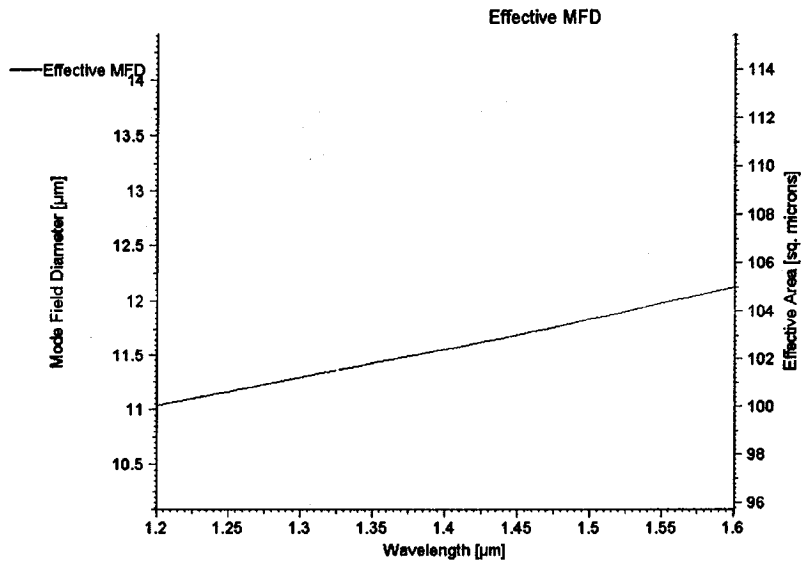

Figure 3.8 Effictive MFD wavelength function1

e) Single mode MFD frequency function

When the diameter of cladding is reduced to 20.5 μm, LP (0,1) mode MFD increases if light wavelength is longer than 1.4 μm. If the light wavelength is shorter than 1.4 μm, its MFD will become smaller than the one of 30 μm cladding diameter fiber(Figure 3.9).

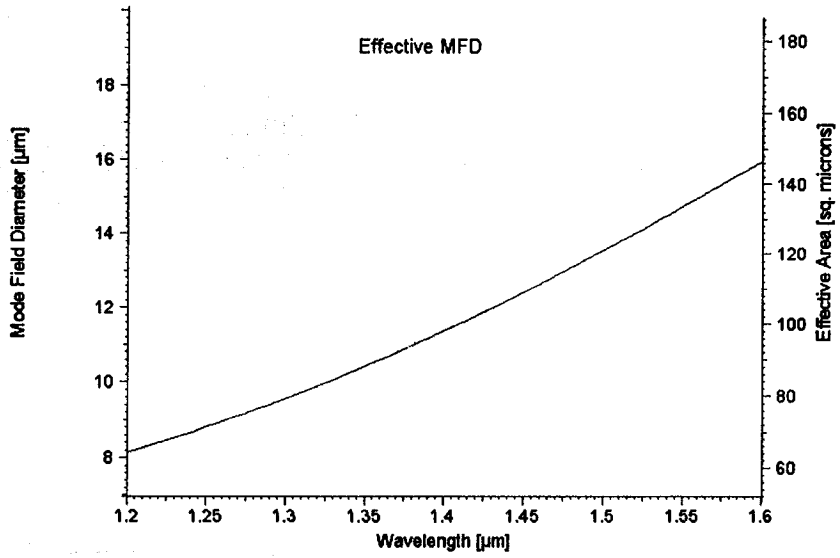

Figure 3.9 LP01 mode MFD

3.2 2x2 Fiber coupler model

When discuss couplers, it is customary to refer to them in terms of the number of input and output ports on the device. For example, a device with two inputs and two outputs would be called a "2x2 coupler." Several useful properties of many optical devices can be obtained by considering the simple case of a 2X2 coupler. Whatever they are fused fibers couplers, planar waveguides or side-polished fiber couplers, much of the

input field propagations outside the original fiber core. By carefully design the coupling region; this decoupled field can be re-coupled into the other fiber .

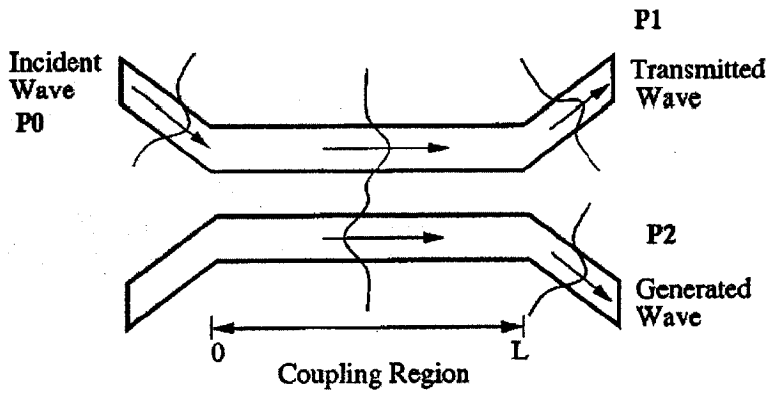

Figure 3.10: Schematic illustration of the scattering process within couplers.[4]

A common fused-fiber-coupler is considered in following analyses. Each input and output fiber has a long tapered section of length w. Here, P_0 is the input power, P_1 is the throughout power, and P_2 is the power coupled into the second fiber (see figure 3.10). As the input light P_0 propagate along the taper area in fiber 1 and into coupling region L, there is a significant decrease in V-number owing to the reduction in ratio r/ λ. Consequently, as the signal enters the coupling region, an increasingly larger portion of the input field now propagates outside the core of the fiber. Depending on the dimensioning of the coupling region, any desired fraction of this decoupled field can be re-coupled into the other fiber. By making the tapers very gradual, only a negligible fraction of incoming optical power is reflected back into either of the input ports. These devices are also known as directional coupler. For polished fiber coupler, one side cladding of the fiber was polished away. Therefore, as input light enters the coupling area, the light field comes outside of fiber core. Then it will be re-coupled into other fibers.

In fused coupler model, the optical power coupled from one fiber to another can be varied through three parameters: the axial length of the coupling region over which the fields from the two fibers interact; the size of the reduced radius r in the coupling region; and Δr, the difference in radio of the two fibers in coupling region. Assuming that the coupler is lossless, the expression for the power P_2 coupled from one fiber to another fiber over an axial distance z is [40]

$$P_2 = P_0 \sin^2(kz) \tag{3.1}$$

$$P_1 = P_0 - P_2 = P_0 \cos^2(kz) \tag{3.2}$$

where k is the coupling coefficient describing the interaction between the fields in the two fibers.

Following simulation results described that the coupled power of this coupler is distributed with the coupling length z in sine function and transmission power of the coupler is distributed with cosine function (see figure 3.11, 3.12).

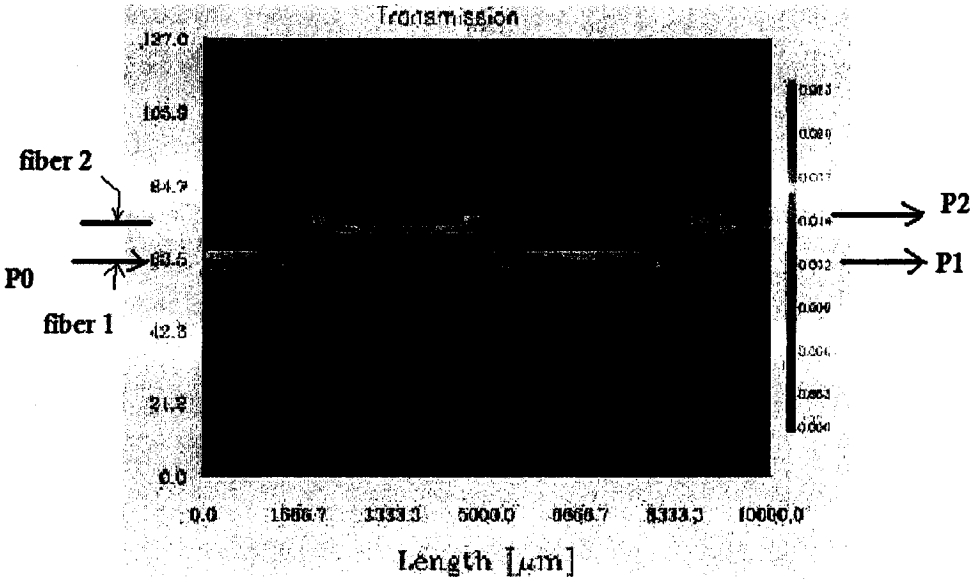

Figure 3.11 Light power distribution in the coupling length

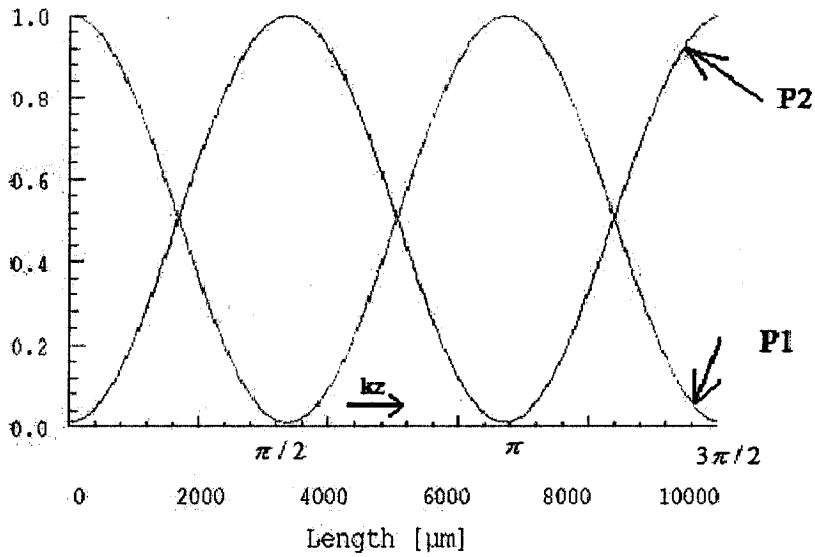

Figure 3.12 Normalized light power distribution

Analogous to fused-fiber-couplers, in the coupling region, the interaction between the guides of waveguide devices can be varied through the guide width w, the gap s

between the guides, and the refractive index n1 between the guides. The transmission characteristics of the symmetric coupler can be expressed as [41]

$$P_2 = P_0 \sin^2(kz)e^{-\alpha z} \tag{3.3}$$

$$k = f(n_1, w, d) \tag{3.4}$$

where w is guide width , α is the optical loss coefficient in the guide, and d is the gap between the guides.

In following simulations, an ideal fiber coupler model is used, which has the same reflective index between the two fiber cores in coupling region. The length of the coupling region was set to a fixed value 1000 μm. The output power is varied with the gap between the two fiber cores.

In Figure 3.13 (a, b), when the gap between the two fiber cores is around 7.4 μm, at the end of coupling area point, kz= $\pi/2$. The coupled power P2 of the coupler reaches its maximum value.

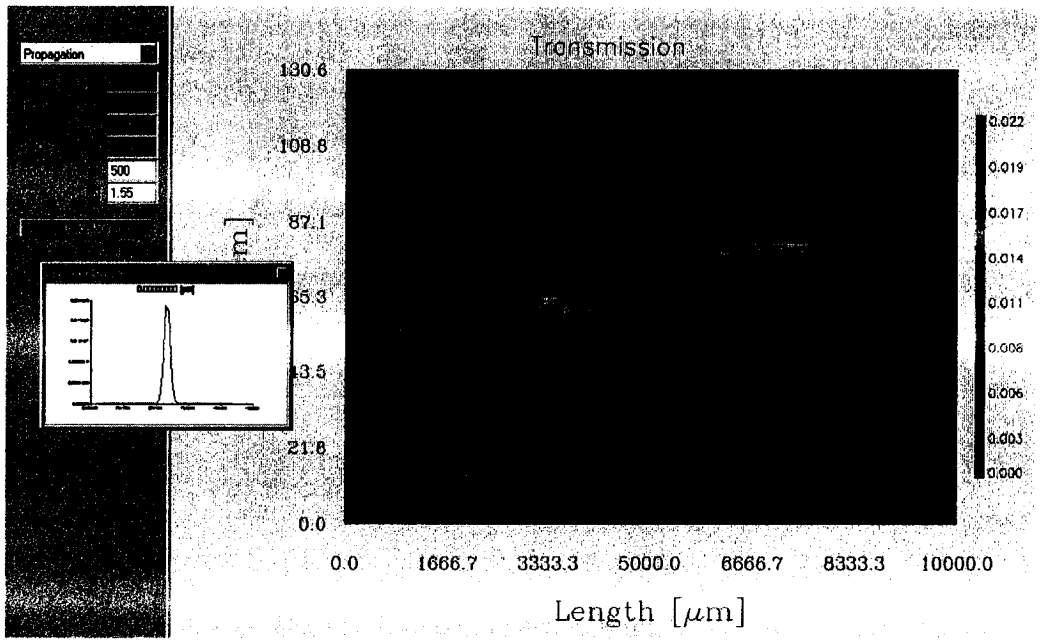

(a)

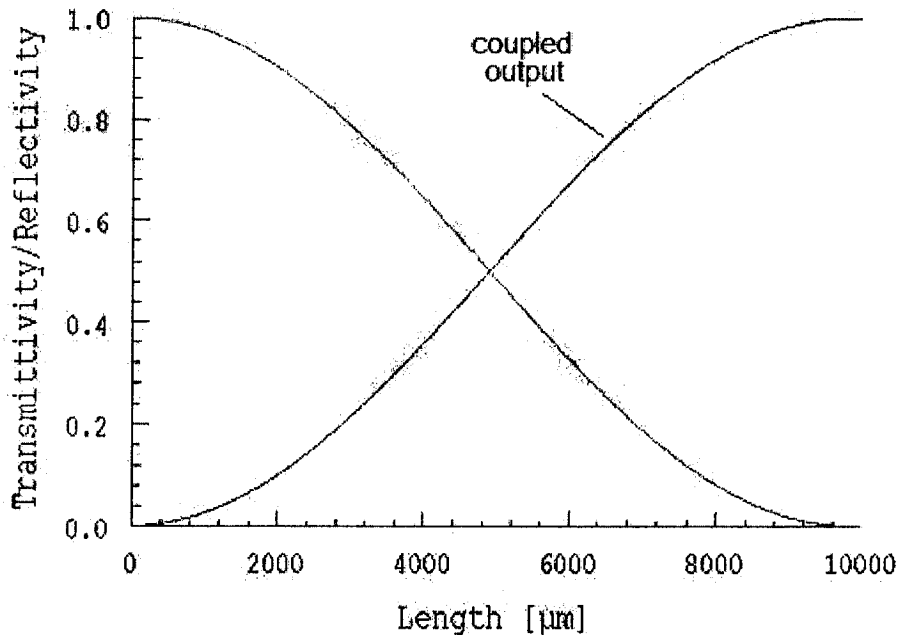

(b)

Figure 3.13 The power distribution when the distance between fiber cores is 7.4 μm (a), (b)

In Figure 3.14 (a, b), when the gap between increases to 8.65 μm, at the end of coupling area point, kz= $\pi/4$, and transmission power P1 is equal to coupled power P2.

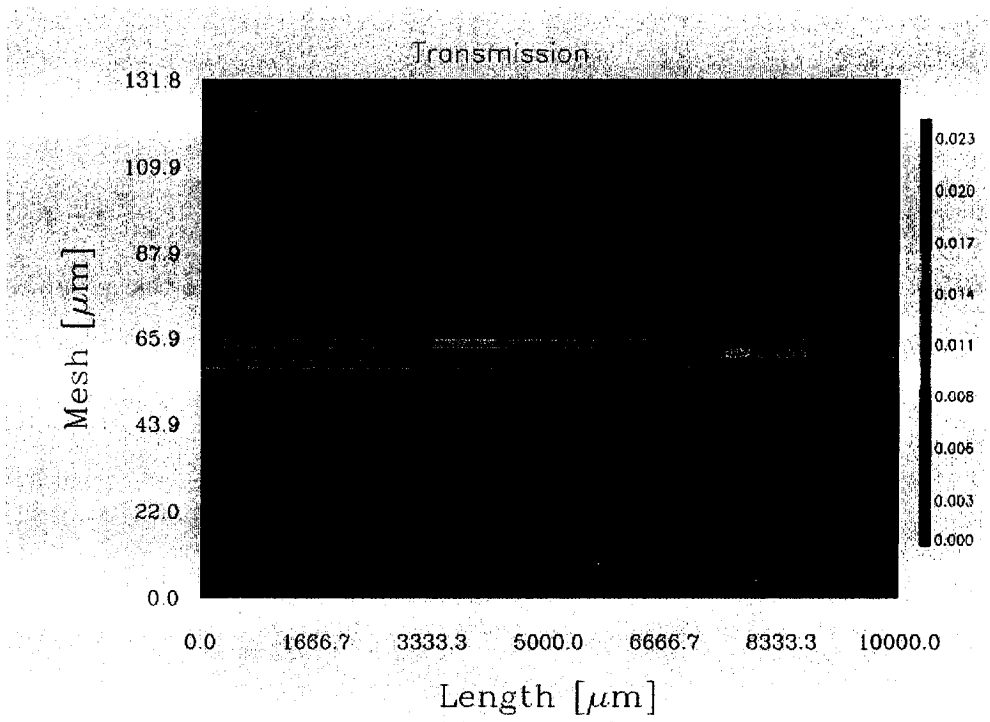

(a)

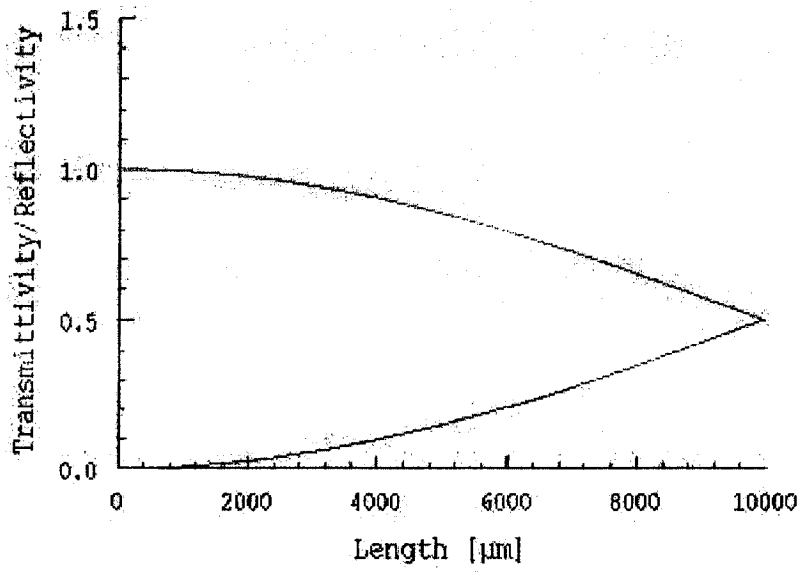

(b)

Figure 3.14 The power distribution when the distance between fiber cores is 8.65 μm (a), (b)

When the gay between the two fiber cores decreases to 5.51 μm, at the end of coupling area point, kz= π. The coupled power in fiber 2 decreases to minimum and the transmission power keep increasing to maximum at same time (figure 3.15).

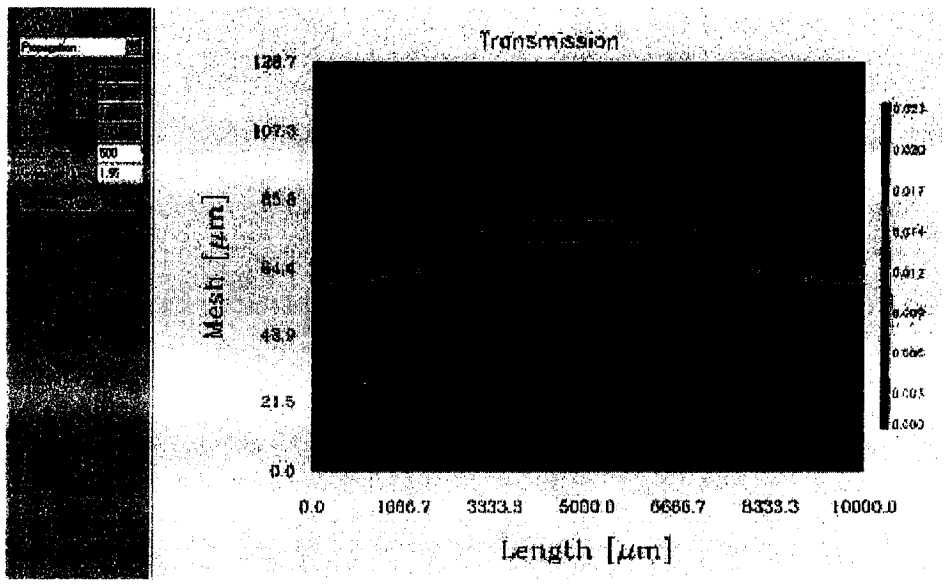

(a)

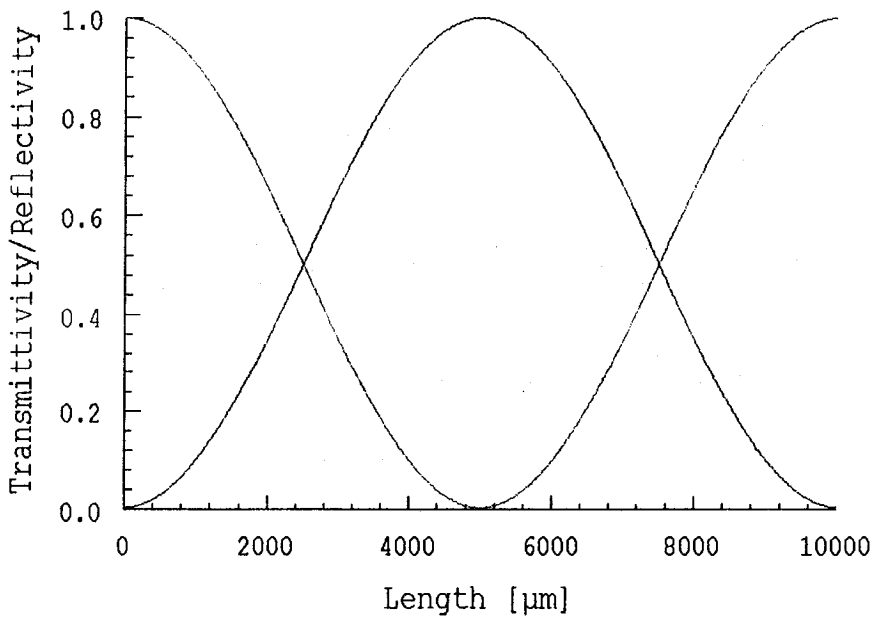

Figure 3.15 The power distribution when the distance between fiber cores is 5.51 μm (a), (b)

When the gay between the two fiber cores decreases to 3.85 μm (figure 3.16), at the end of coupling area point, kz= $3\pi/2$. The coupled power in fiber 2 increases again to next maximum value, and the transmission power decreases to minimum at same time.

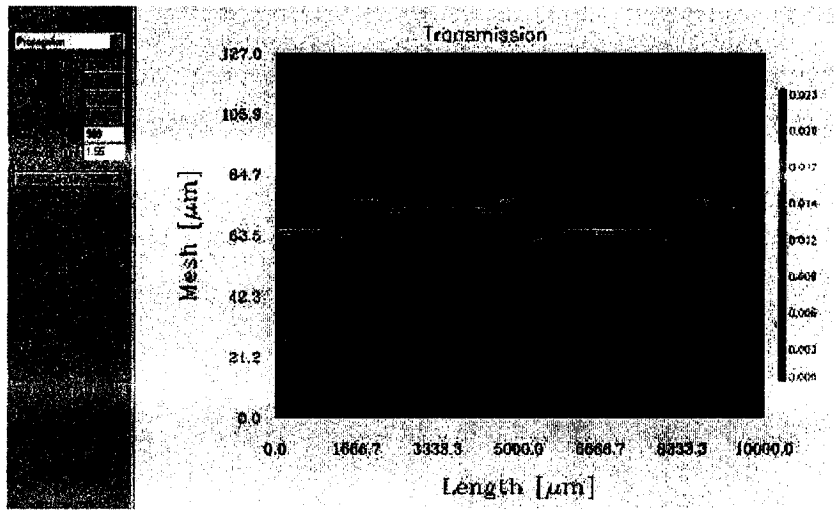

(a)

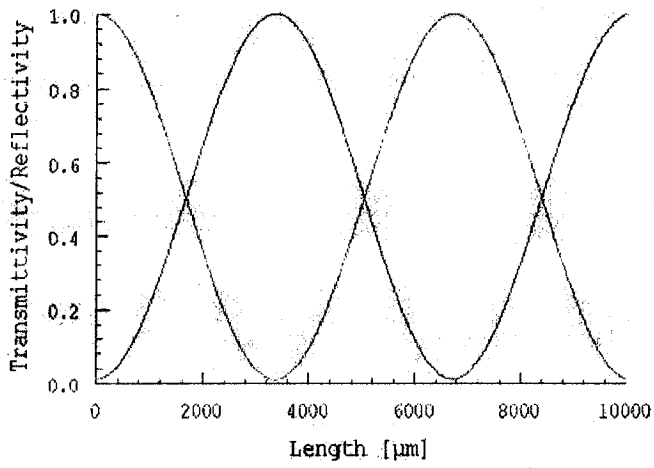

(b)

Figure 3.16 the power distribution when the distance between fiber cores is 3.85 μm (a), (b)

In Figure 3.17, all coupled power in fiber 2 display together, we will see P2 normalized power is varied with the gap distance between the two fiber cores in coupling region.

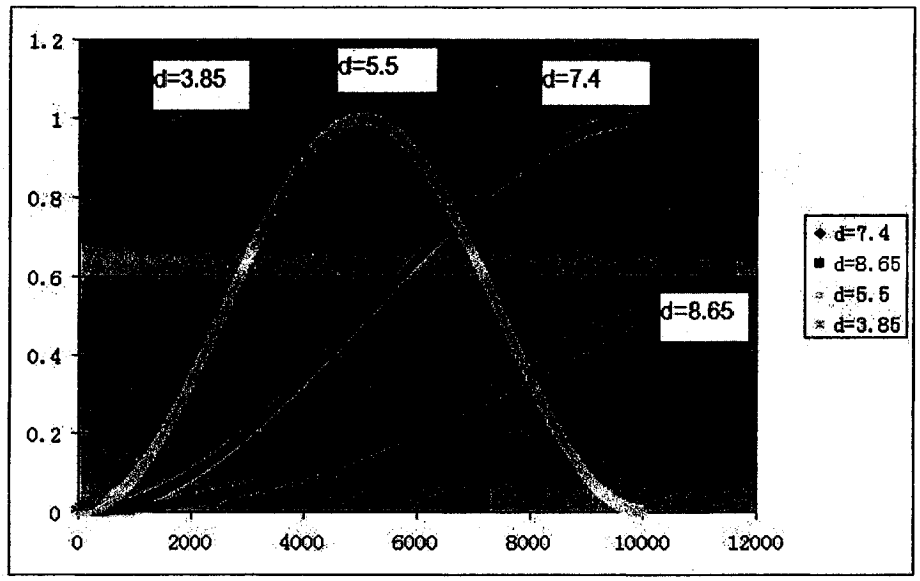

Figure 3.17 The ratio of transitivity and reflectivity of light power in the coupler

The next table is the relations between gap d of the two fiber cores and coupling coefficient. It is an approximate exponential function (in Figure 3.18).

$$k = f(n_1, w, d) = \beta(n_1, w)e^{-qd} \tag{3.5}$$

d (μm)	k (μm-1)
3.85	0.000471239
5.51	0.000314159
7.4	0.00015708
8.65	7.85398E-05

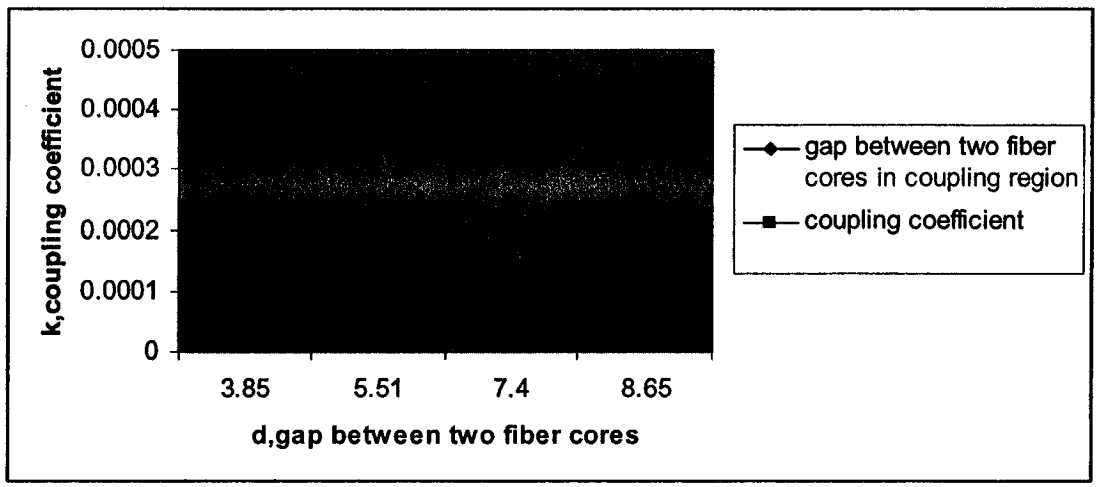

Figure 3.18 coupling coefficient, k varies with the gap between the fiber cores

3.3 Simulation a fiber coupler with FBG

Here is the fiber coupler model with fiber Bragg gratings (FBG). Since FBG fiber has depicted refractive index grating in its core, a specific wavelength would be reflected back while other wavelength go through the fiber.

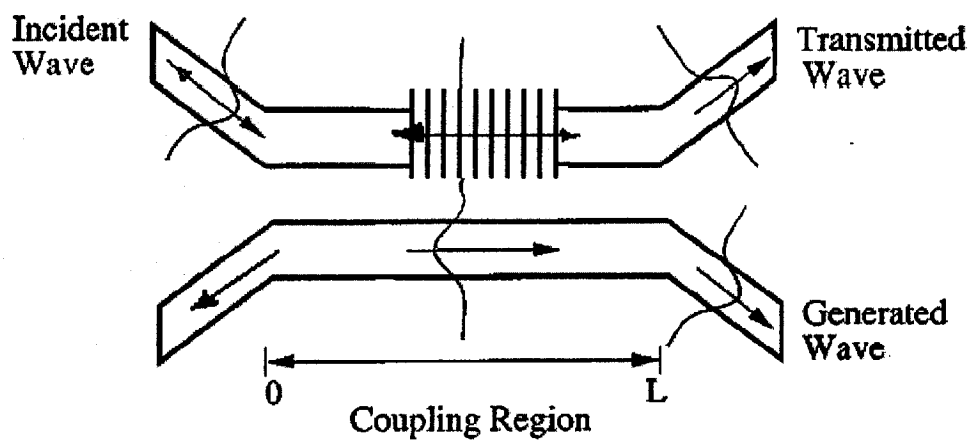

Figure 3.19 fiber coupler with FBG sketch

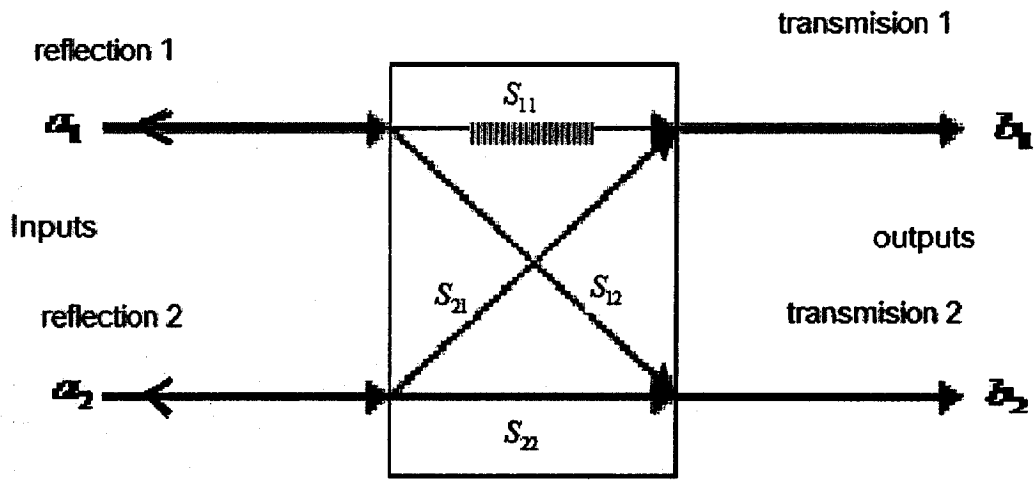

Figure 3.20 fiber coupler module with FBG

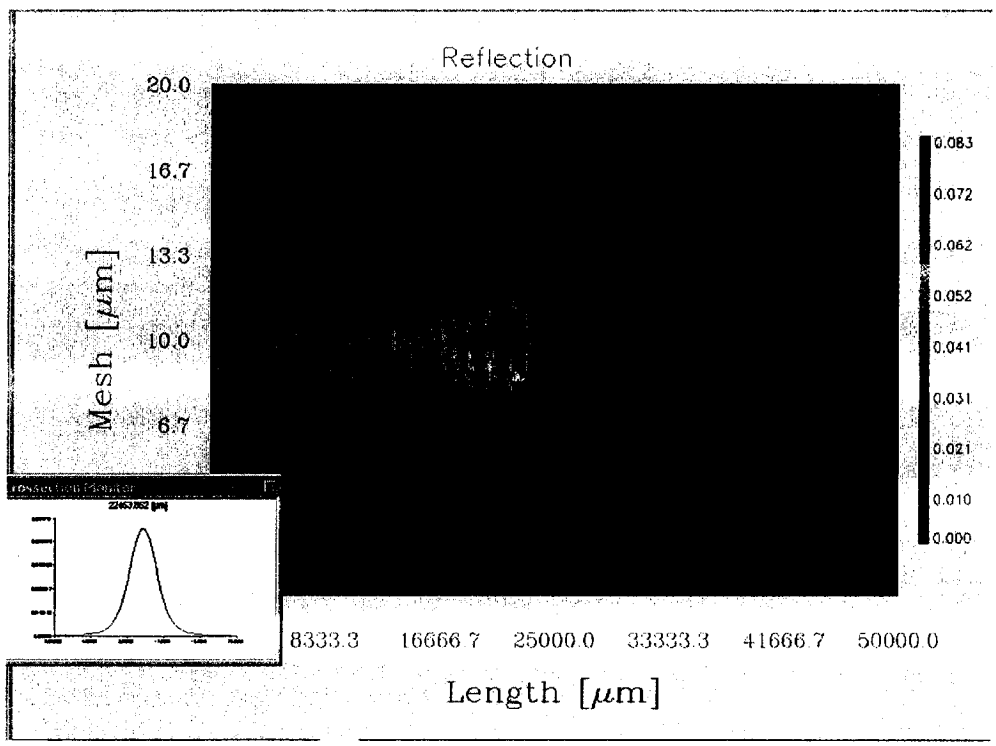

Figure 3.21 FBG fiber coupler reflection

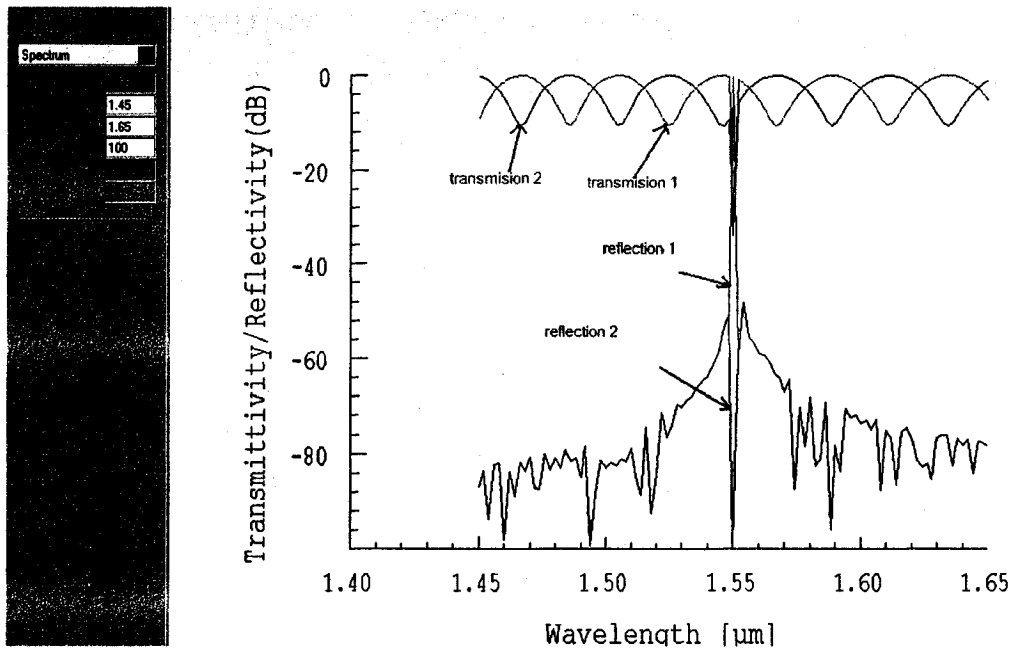

Figure 3.22 the spectrum map of coupler with FBG

In FBG fiber coupler simulation, a normal FBG (1550nm) is used in the coupler. From Figure 3.22, we know the most 1550nm light power will reflect to reflection 1 (the fiber itself). If we want get the 1550nm signal from port 4, a special FBG with lower reflection and high cladding reflective mode is more suitable than the normal one, for example, a long period fiber grating or tilted (taped) Bragg Grating.

CHAPTER 4

DESIGN AND FABRICATION

INTRODUCTION

In this Chapter, the design and fabrication of V-grooves, side-polished fibers, and fiber couplers are introduced. Figure 4.1shows side-polished fiber couplers fabrication processes as following:

Step 1: P type Silicon substrates are used to grow a layer of S_iO_2 by Wet Oxidation.

Step 2: samples are coated with Positive Photo resist (PR+).

Step 3: The exposed PR+ is developed and removed by dipping the samples in a solution of developer.

Step 4: the layer of S_iO_2 is etched away by using HF:NH_4F and HF:H_2O solutions.

Step 5: PR+ is removed by dipping them in an Acetone filled beaker.

Step 6: Silicon V-grooves are etched by using 25%TMAH under 90C°.

Step 7: Prepared fibers are put and sliced into the V-grooves.

Step 8: The fibers are side-polished by using fine sandpapers.

Step 9, 10, and 11: Two samples are put face to face to make a side-polished fiber coupler.

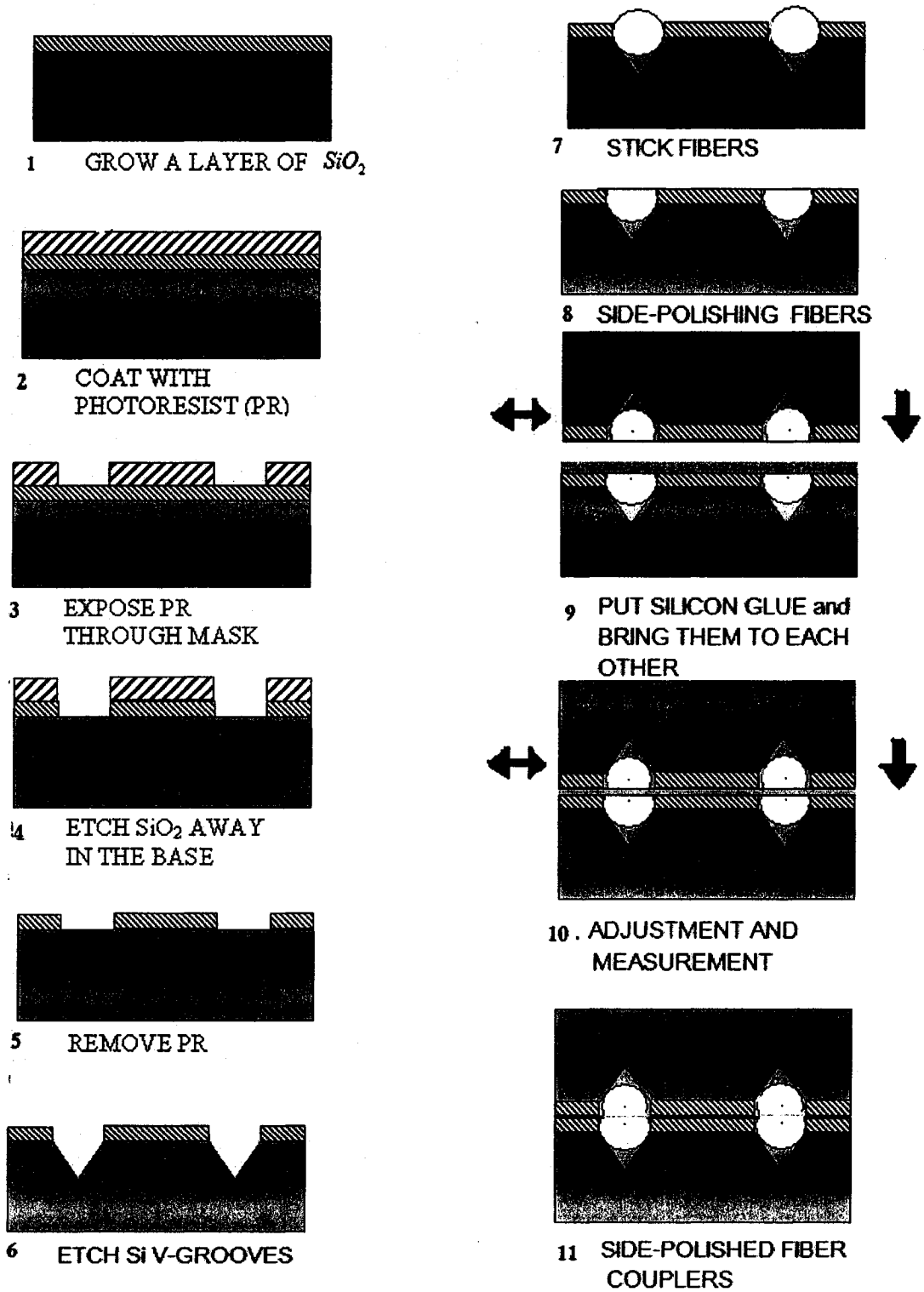

Figure 4.1 side-polished fiber couplers fabrication processes

4.1 Design of V-grooves

From section 2.5, we know that V-grooves could be etched by TMAH solution on P <100> wafer with specific angle θ=54.74°. Figure 4.2 shows the V-groove and fiber sectional sketch map. The following calculations are used to get the relationship among the width of V-grooves, L, the width of polished fiber, W, and the depth of the V-grooves, H.

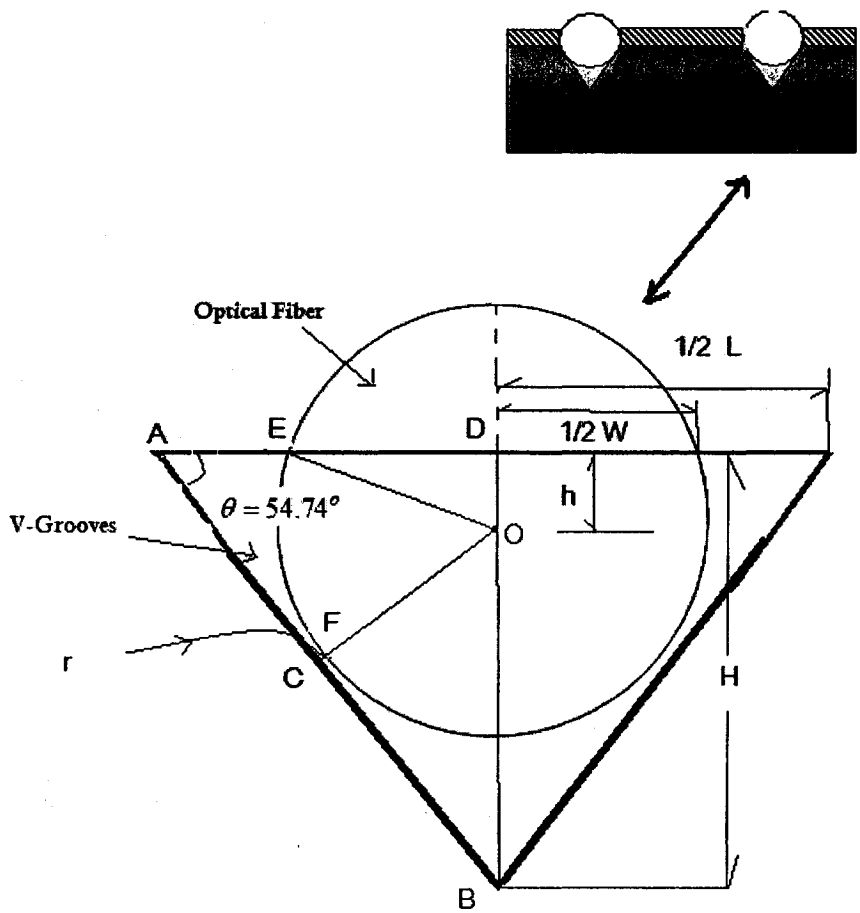

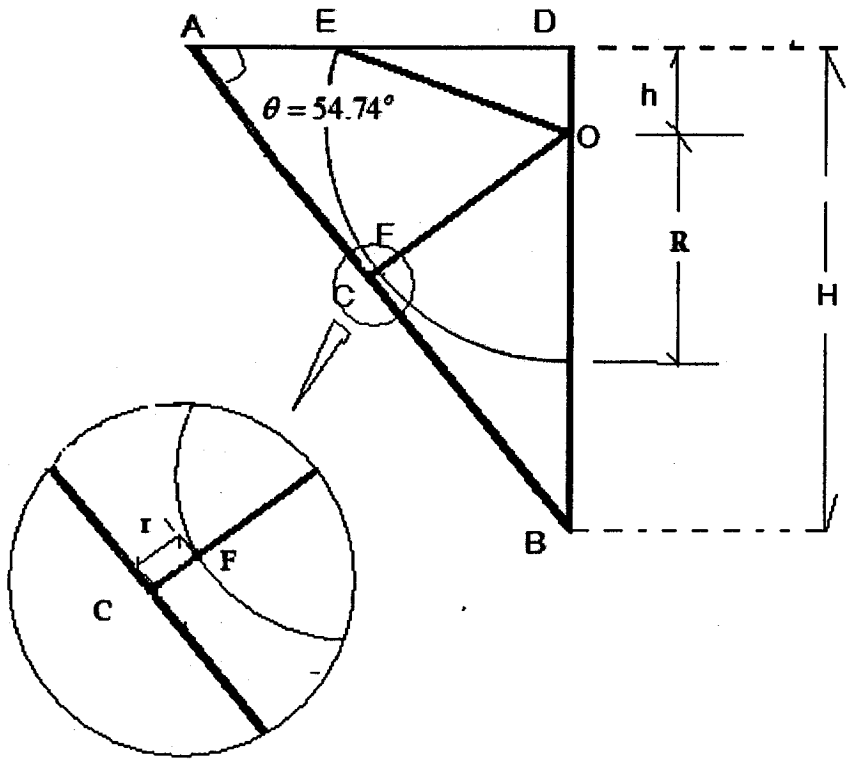

Figure 4.2 V-grooves and fiber sectional sketch map

From the above figure 4.2, by mathematic calculations, we see that:

$$H = \frac{1}{2} L \tan\theta = \frac{1}{2} \frac{sin\theta}{\cos\theta} L \tag{4.1}$$

$$h = H - \frac{(R+r)}{\cos\theta} = \frac{\frac{1}{2} L \sin\theta - (R+r)}{\cos\theta} \tag{4.2}$$

$$W = 2\sqrt{R^2 - h^2} = 2\sqrt{R^2 - [H - \frac{(R+r)}{\cos\theta}]^2} = 2\sqrt{R^2 - \left[\frac{\frac{1}{2} L \sin\theta - (R+r)}{\cos\theta}\right]^2} \tag{4.3}$$

$$H = h + \frac{(R+r)}{\cos\theta} \tag{4.4}$$

Here for P<100> Silicon wafer $\theta = 54.74^{\circ}$ after V-grooves are etched in TMAH, r is the small gap between fiber and V-groove which was filled by a special silicon glue. It is assumed that r= $2\mu m$, and R, the fiber radius, is about 62.5 μm.

Therefore, it is easy to get the relationship between h and L, and W and L, where $H = h + \frac{(R+r)}{\cos\theta} \approx h + 11.7 \ \ \mu m$. For example, in Figure 4.3 and 4.4, they give us the relationship between W (width of the polished fiber plane) and L (width of the V-grooves), and between h (the distance from the center of fiber to the polished plane) and L. Figure 4.4 gives us an example of the three parameters h, W, and L. If we want to get a polished SM fiber which the polished plane is close to the core of the fiber, h is about 4 μm. Then, from the figure 4.4, we got L, the width of the V-grooves on P <100>, is about 164 μm and W, the width of the polished plane of the fiber, is about 124.8 μm.

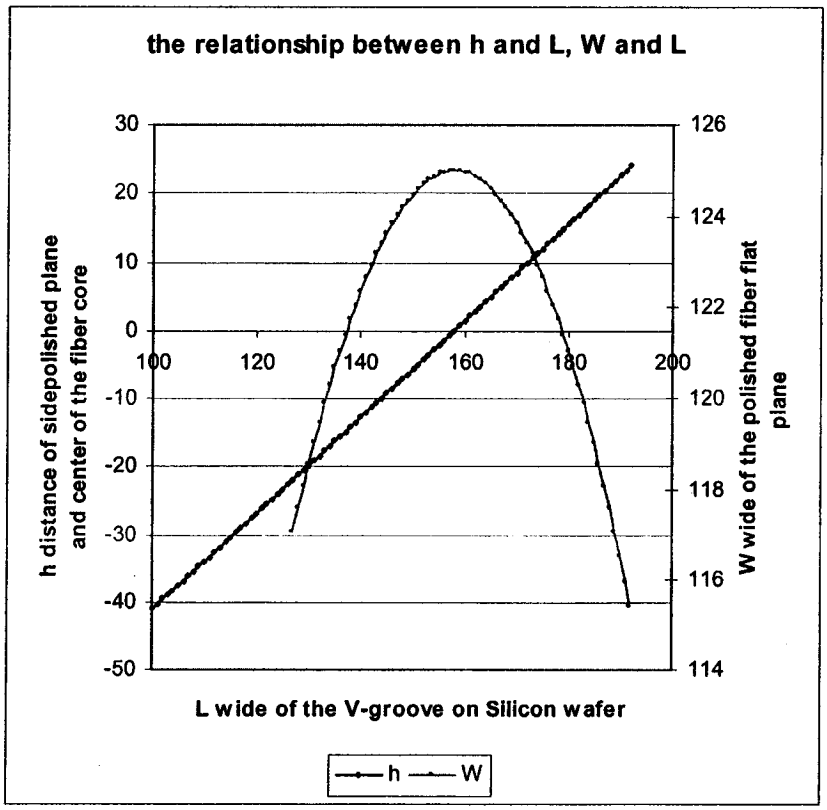

Figure 4.3 The relationships among parameters of h , L, and W of side-polished fiber in V-grooves

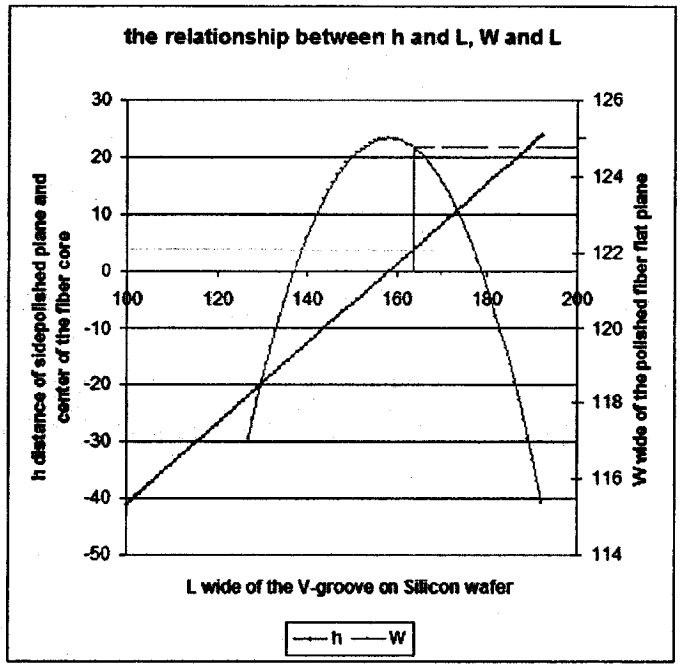

Figure 4.4 an example of the three parameters h, L, and W (h=4, L=164, W=124.8)

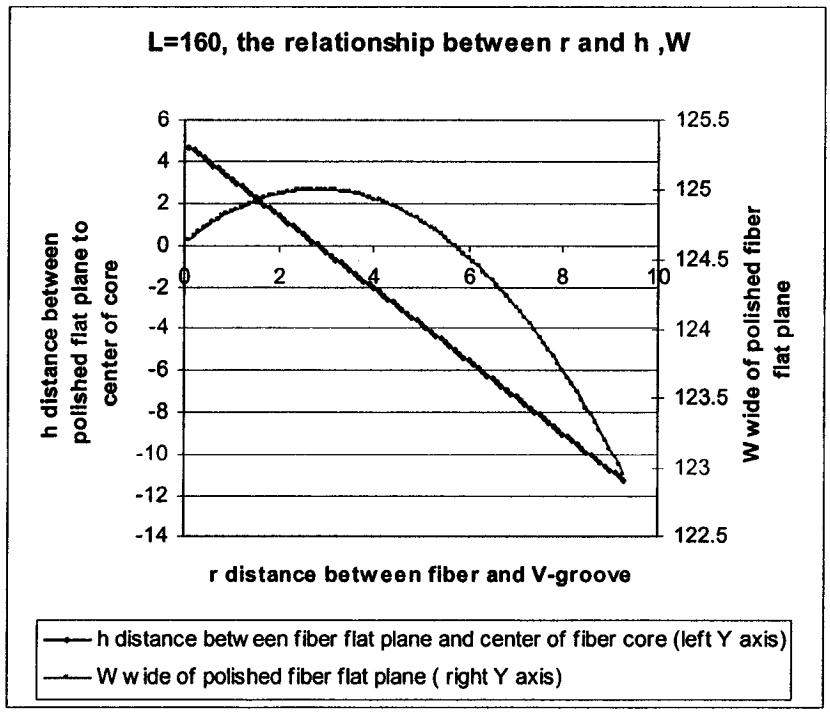

Figure 4.5 relationship among h, r, and W (L=160)

As it is shown in figure 4.5, if r is between 0.1~0.3 μm, h is about 4 μm to 4.5 μm when V-grooves width is about 160 μm. That means almost all of the cladding of the fiber was polished away, and the fiber core is very close to the side-polished plane. The depth H of the V-grooves is about 116 μm.

The Silicon etching time in TMAH can be calculated from $t(\min) = \frac{H}{K}$, where K is about 0.6 μm/min for P <100> Silicon in 25% TMAH at 90 $^{\circ}C$. Therefore, the time for etching a V-groove with a width of 160 μm is about

$$t = \frac{H}{K} = \frac{116}{0.6} = 193.3\min = 3.22 hours.$$

Masks for V-grooves with width of 160 μm, 180 μm , 200 μm , 280 μm and 300 μm , were designed and fabricated in the lab.

4.2 V-grooves Fabrication

4.2.1 Etching V-Grooves in Silicon

25% concentration of TMAH was used in the experiment for making the V-grooves. The TMAH anisotropic etching is considered by the fact that <111> family planes confine the etching advancement since the etch rate of <111> planes is much lower than that of any other plane. Figure 4.8 is the TMAH etching experiment set-up. The bottom of the samples should be covered with SiO_2 which could protect the back side of the Silicon sample in TMAH.

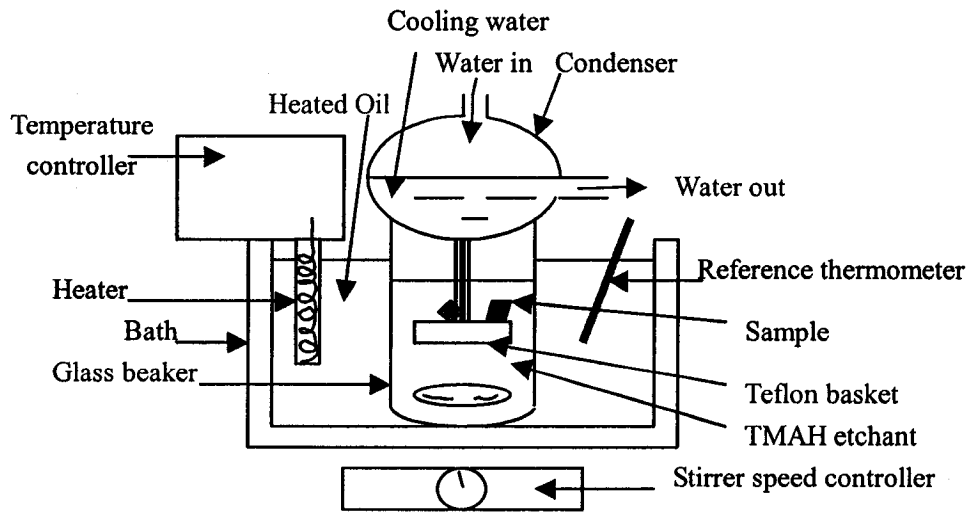

Figure 4.6 TMAH etching Set-up [28]

Figure 4.7, 4.8 and 4.9 are the SEM pictures of the V-grooves which was etched by 25% TMAH for about 3.5 hours at 90 $^{\circ}$C (160 μm mask).

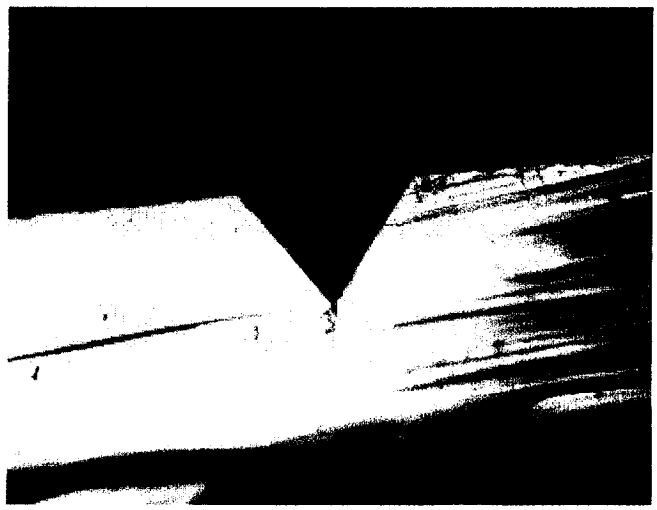

Figure 4.7 V-grooves microscope picture (L=160 μm mask and etching 3.5 hours)

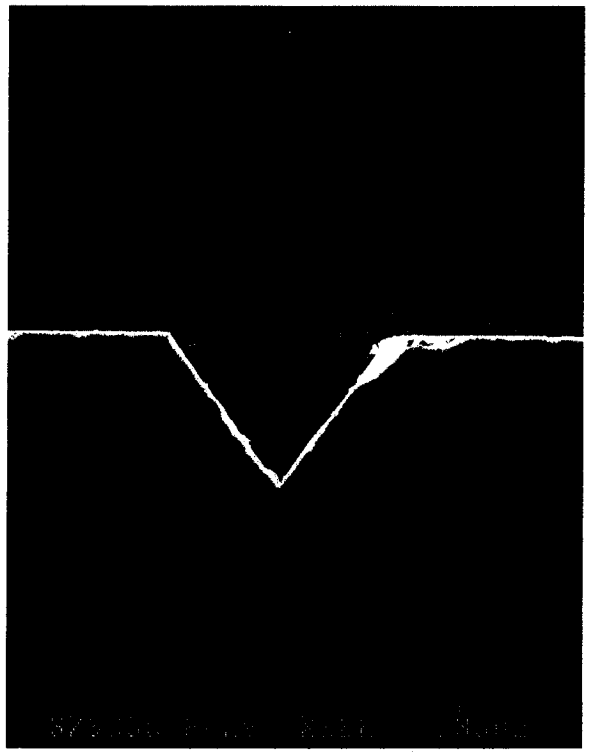

Figure 4.8 SEM picture of the V-groove

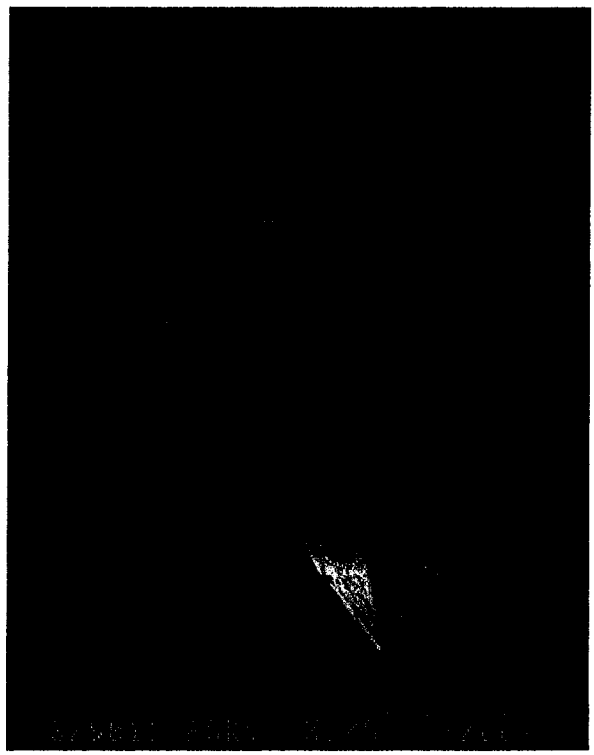

Figure 4.9 SEM picture of top view of the V-groove

4.3 Side- polished fibers and couplers fabrication

4.3.1 Polishing the fibers

Once V-grooves are made, fibers without coating were stick into these V-grooves to make the sample. Special silicon glue was used to stick fibers into V-grooves. Figure 4.10(a) is the microscope picture of V-groove section with a width of 160 μm.

(a) (b)

Figure 4.10 sample preparing (a), (b)

In order to polish these fibers in the sample equally, a plane was made with a smooth glass plane and two silicon samples (see figure 4.11 (a)). The V-groove sample with fibers was put between the two silicon wafers.

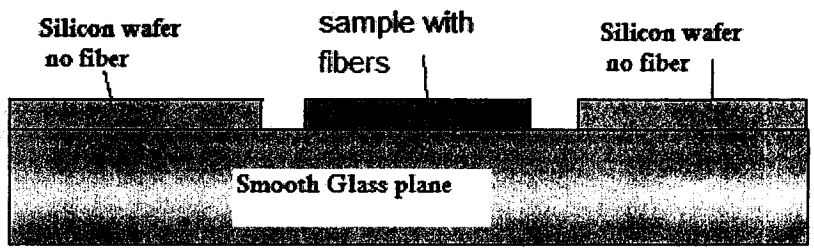

(a)

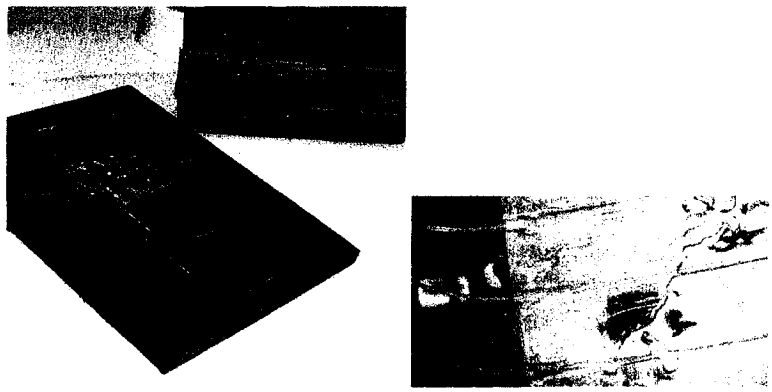

(b) (c)

Figure 4.11 Glass plane (a, b), side-polished fiber picture (c)

4.3.2 Improvement of the processes of fiber-polishing

At the beginning, the fibers were easy broken either in the V-grooves and the edges of wafer sample (figure 4.12).

(a) (b)

Figure 4.12 (a) Broken fibers in the middle of V-Grooves (b) at the edges of the sample

Two steps of sticking fibers on sample are used to improve the polishing process. First, 5 minute silicon Epoxy glue was used in sticking fibers into V-grooves. Once the glue in V-groove was frozen, fibers with bend were made at the edges of sample and coved with glue in order to get enough protection.

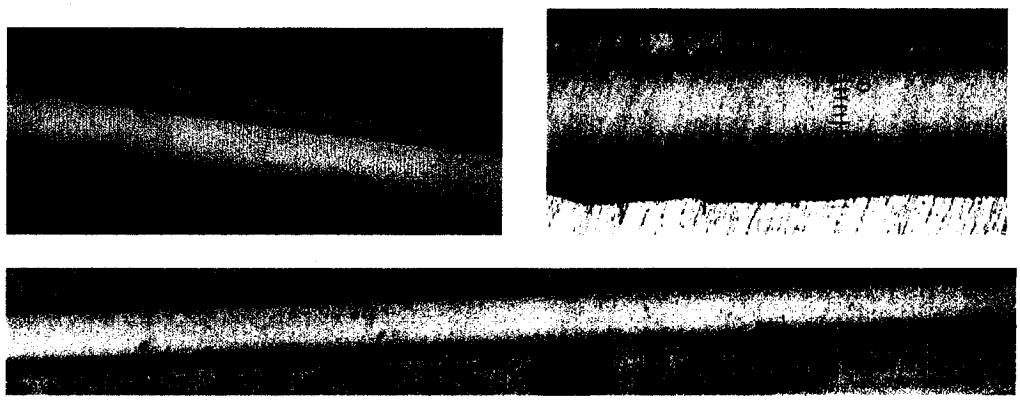

Figure 4.13 well polished fibers in the middle of V-Grooves

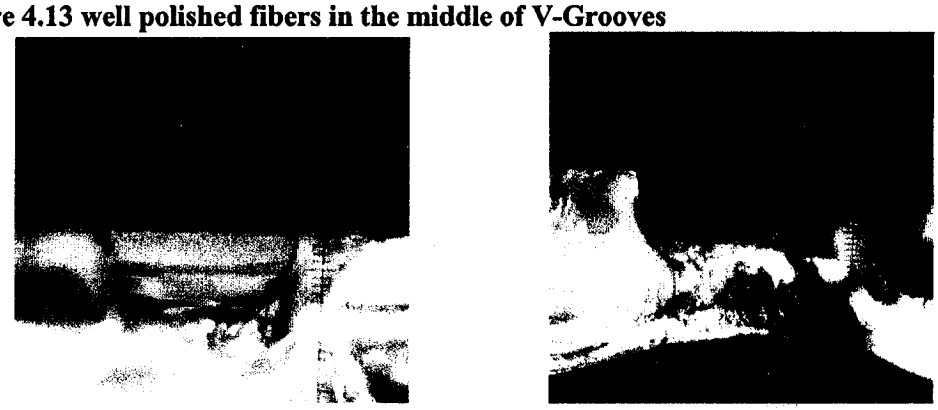

Figure 4.14 well polished fibers section pictures in the V-Groove of microscope

4.3.3 Coupling the fibers

From the figure 4.15, we see that there is a small gap between the two polished fibers since the polished planes in these fibers were not perfect. Liquid Silicon glue with similar RI as glass was used between the two fibers.

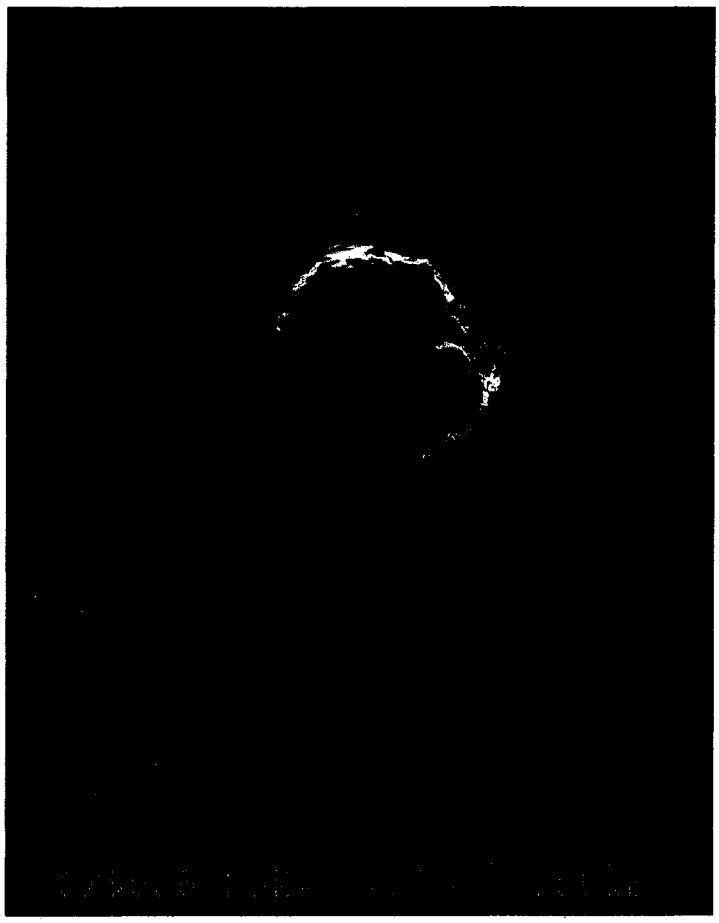

Figure 4.15 SEM picture of the fabricated fiber coupler

As we can see there is a small angle $\angle\phi$ between the two fiber symmetrical axes. The distance between the two fiber cores is OO'.

$$OO'=\frac{(h1+h2)}{\cos\angle\phi} \tag{4.7}$$

When the angle $\angle\phi$ is very small, OO' is equal to h1+h2 approximately.

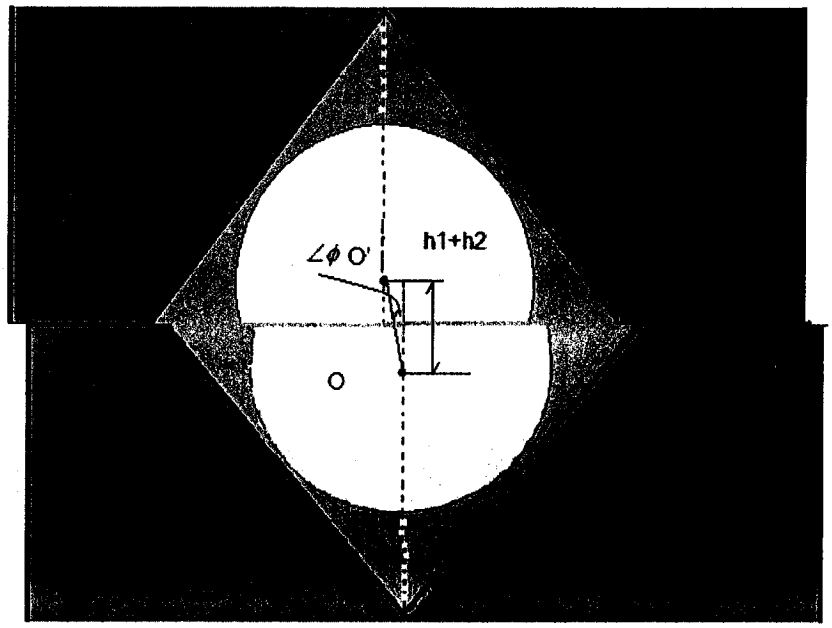

Figure 4.16 Section sketch map of two side-polished fibers coupler

4.3.4 Glass substrate and side-polished fiber star couplers

In order to observe fibers from top in experiments when two samples were put together, glass substrates with some etched ditches were used to hold these well-polished fibers. These well-polished fibers were token off from V-grooves carefully after they were put in Acetone for hours. These fibers were mounted into these ditches of the glass substrate. Figure 4.18 and 4.19 show the sketch maps of fiber coupler with glass substrates. Then, they will be coupled with other samples under microscope. Figure 4.20 is the top view picture of coupler with glass substrate.

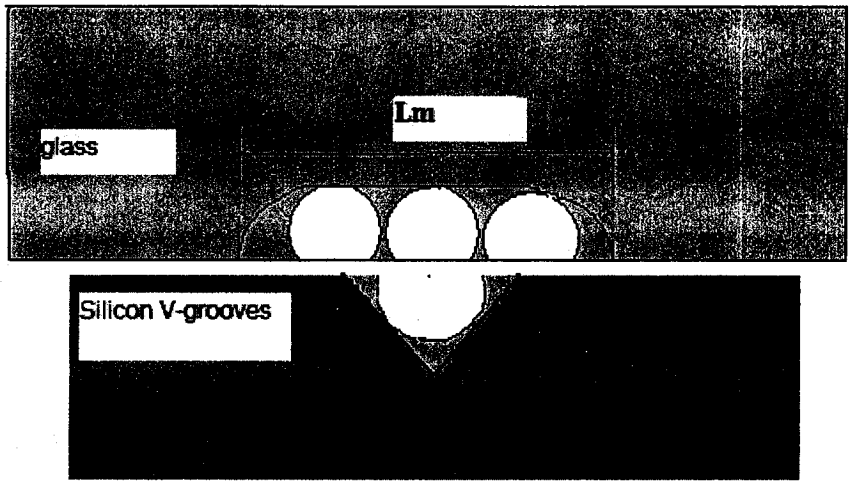

Figure 4.18 a star side-polished coupler with a glass substrate and a silicon V-groove

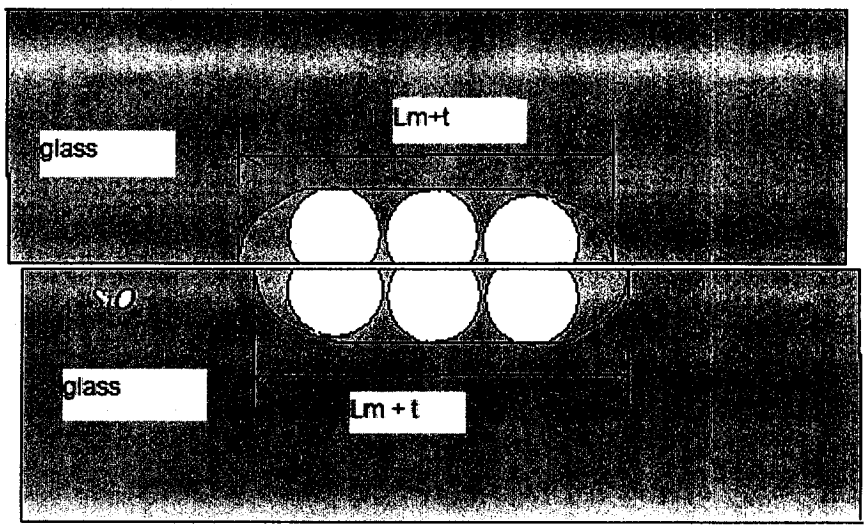

Figure 4.19 a star side-polished coupler based on glass substrates

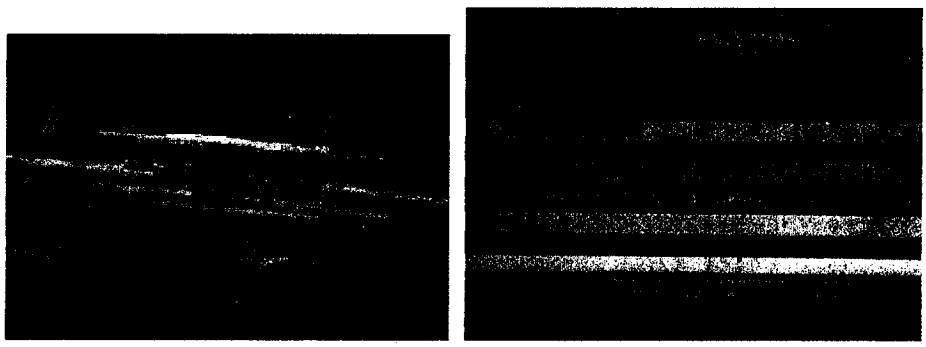

Figure 4.20 a star side-polished coupler sample on a glass substrate

4.4 Couplers with etched fibers

4.4.1 Etched fiber star-coupler design

As we introduced in chapter 3, etched SM fibers also could be used to make couplers. Light input from fiber B, will be coupled to both fibers A and C (figure 4.21). As these fibers should be etched to smaller sizes, one of the challenges to build these couplers is to set the ditch etched in Silicon wafers without damages.

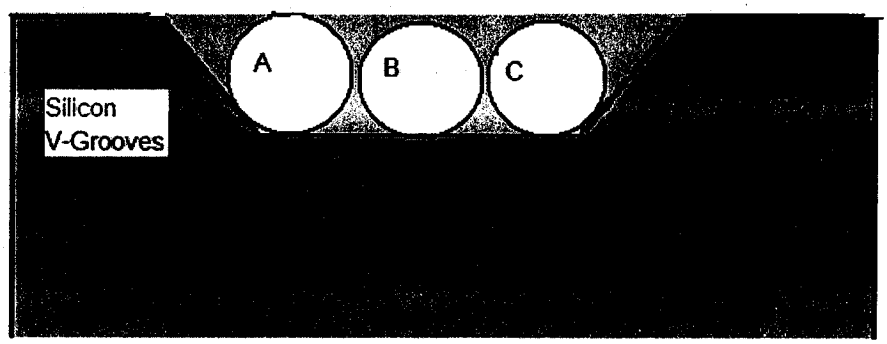

Figure 4.21 the star coupler sketch map of etched fiber star-coupler

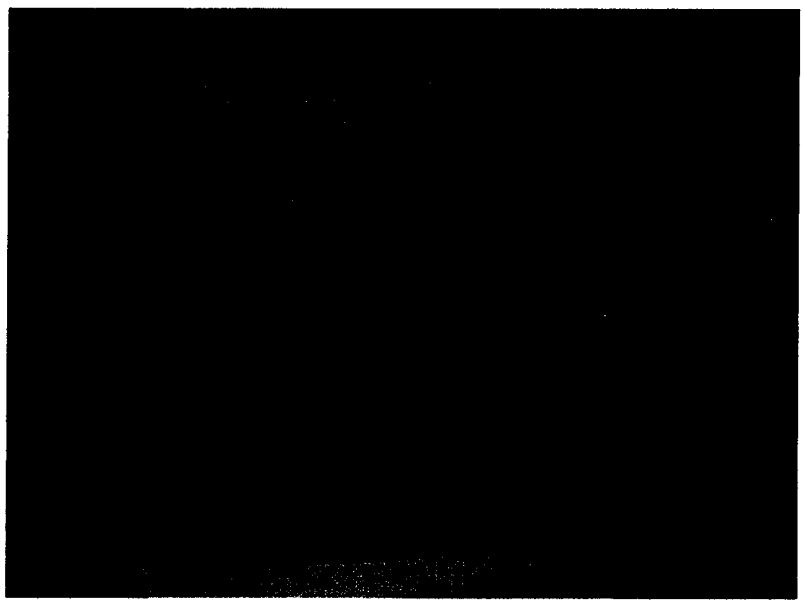

Figure 4.22 SEM picture of wafer (P<100>) after 3.5 hours etching

HF (48%-52%) is used to etch a normal SM fiber to different diameter by time control. For example, after etching 15 min, the SM fiber reaches 80 μm in diameter, and in 32min it reaches to 20 μm in diameter.

Figure 4.23 shows the sketch map of a etched fiber coupler. Two etched fibers were gotten through the shrinking tube. In principle, the light in one of the input fibers will be coupled into the other fiber after the light goes thought the coupling area in the tube. A plastic syringe was used to add silicon glue into the shrink tube before it was heated. Two of these couplers were made in lab (figure 4.24); however, we could not detect any coupling light in the both of output fibers.

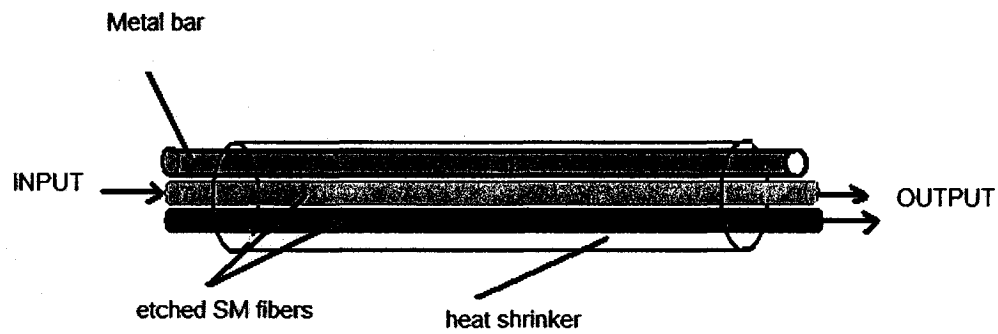

Figure 4.23 SM fiber coupler design 2

Reason analyzing: one of the reason is these fibers were damaged in middle of the tube since these etched fiber filaments were too thin to be put into the heat shrinking tube. The other reason is the distance between the two fiber cores is farer than we expected.

Figure 4.24 etched SM fiber couplers

Comparing with heat shrinkable tube coupler (figure 4.23, 4.24), an etched ditch on Silicon P<110> is easier to handle to make a SM coupler. From section 2.5, P<110> Silicon samples could be etched by TMAH to make such a ditch in figure 4.25.

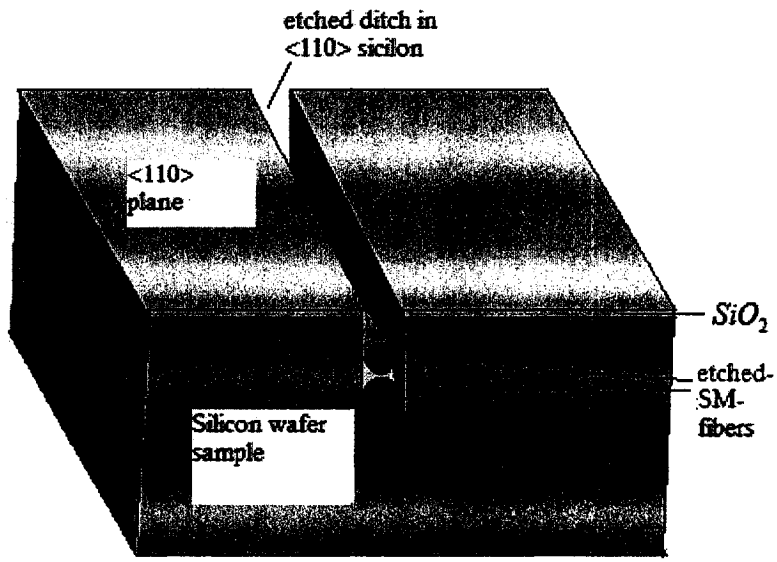

Figure 4.25 the ditch used as a coupling tool of etched SM fiber couplers

4.4.3 Etching fiber from one side

To solve the way handling such thin etched fibers, we try to etch fibers from side. Different methods and processes were used in side fiber etching. For example, One single fiber was covered with PR+ and exposed under UV light, then etching in HF: NH4F. In figure 4.26, the left part of the fiber was covered with PR+, and the rest was the side-etched fiber.

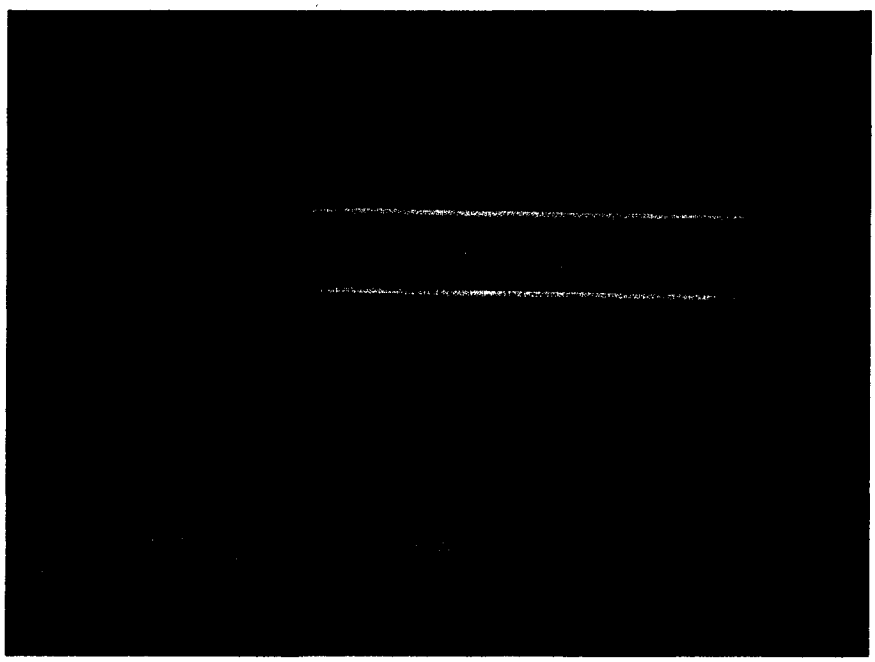

Figure 4.26 side etched SM fiber (the red part is photo resister)

Another process is that bare fibers were put on a smooth PR+ covered Silicon sample (figure 4.27). By controlling the thickness of the PR+ on the sample, the top of the fiber was open while the rest is coved by PR+.

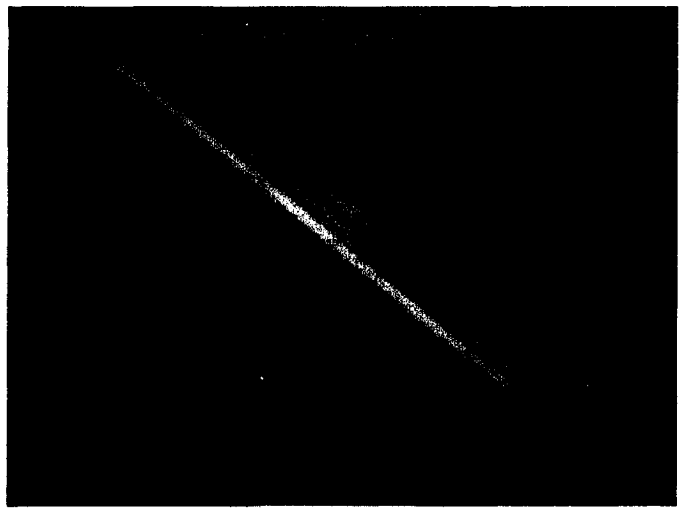

Figure 4.27 Top etched SM fiber

4.4.4 Etched period ditches on fiber

The fiber with etched period ditches also could be used to make couplers (see figure 4.28). Since the part of etched period ditches is very close to the fiber core, it is possible to create a SM fiber coupler by etched grating fibers as well as keeping strong mechanical characteristics of fiber. Figure 4.29 shows the SM fiber which was etched with period ditches. The same process was used to etch side-polished fibers in etching period ditches in their polished planes (figure 4.30).

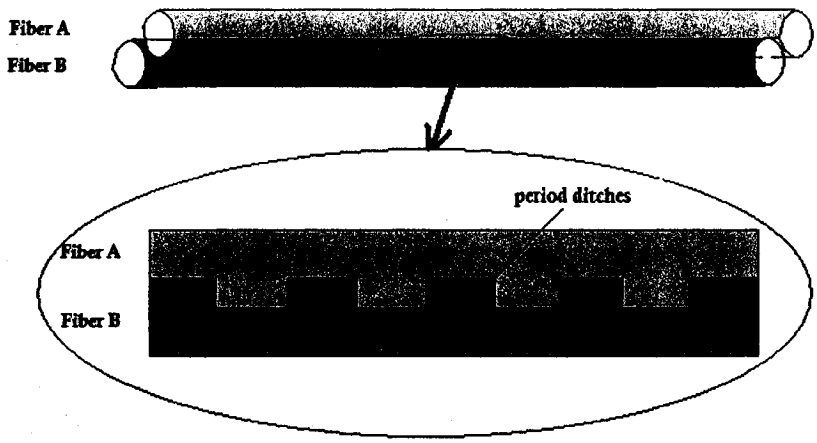

Figure 4. 28 coupler model of fibers with etched period ditches

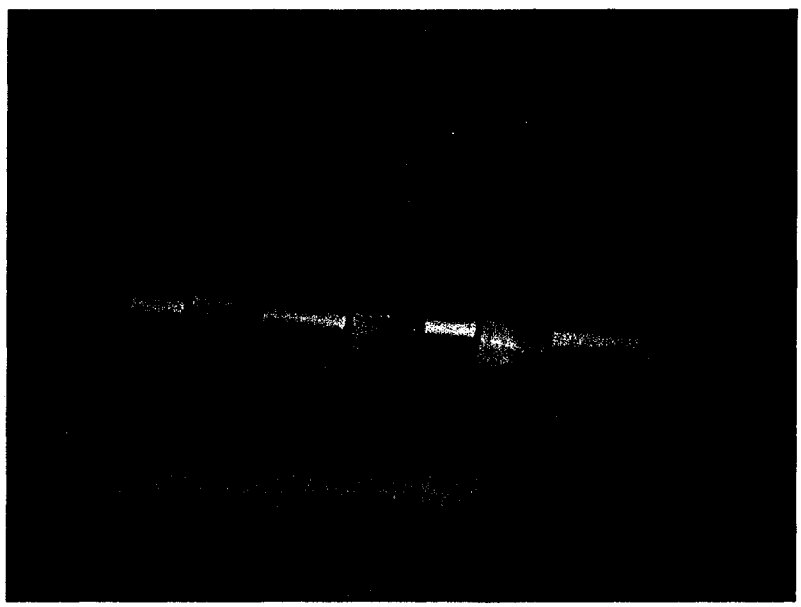

Figure 4. 29 Etched period ditches in a SM fiber

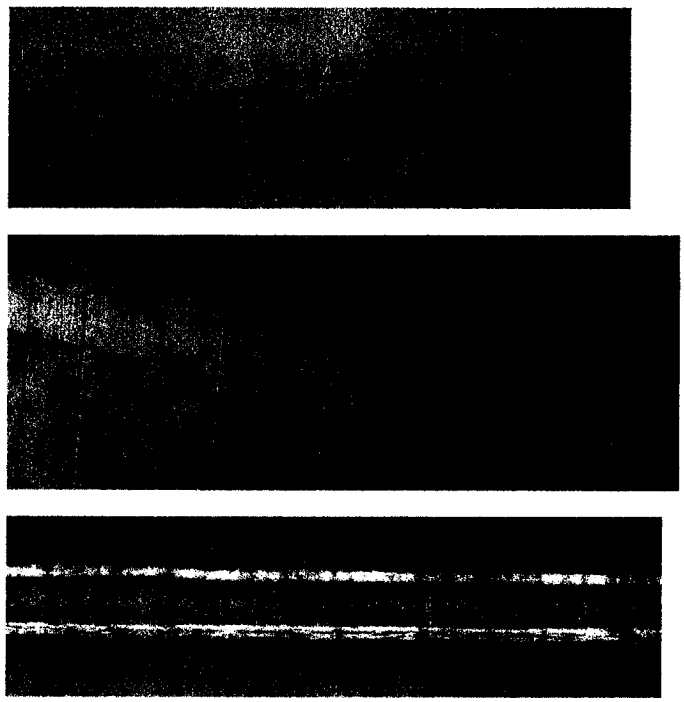

Figure 4. 30 Etched period ditches in side-polished plane of SM fibers

CHAPTER 5

EXPERIMENTS AND APPLICATIONS

INTRODUCTION

In this Chapter, two kinds of couplers, 2x2 coupler and star couplers, were used in these experiments.

5.1 Experiments set up

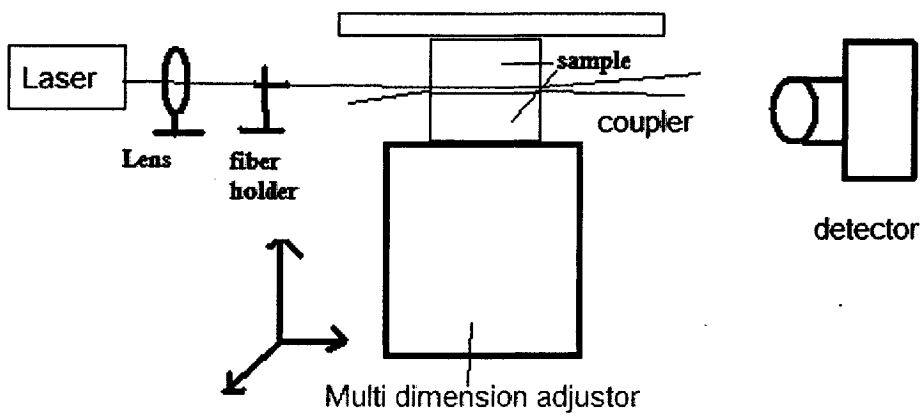

Figure 5.1 experiments set up sketch map

5.1.1 Multi-dimension adjustor

In order to couple two polished fibers, we designed the work stage for fiber coupler as in figure 5.2, a coarse horizontal X-Y stage and a vertical Z coarse stage, and a small fine XYZ stage is used to adjust the sample in μm level (figure 5.3).

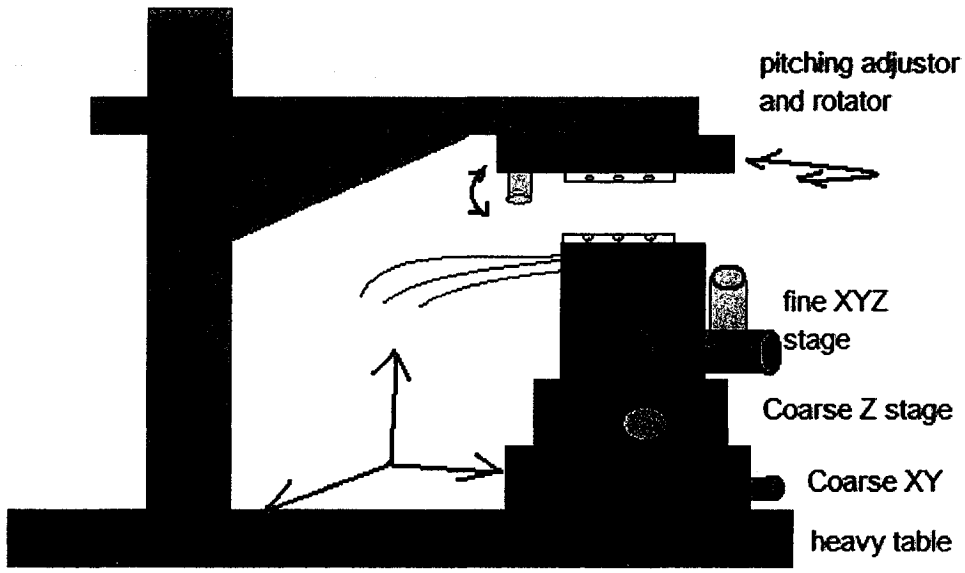

Figure 5.2 Sketch of coupling work stage

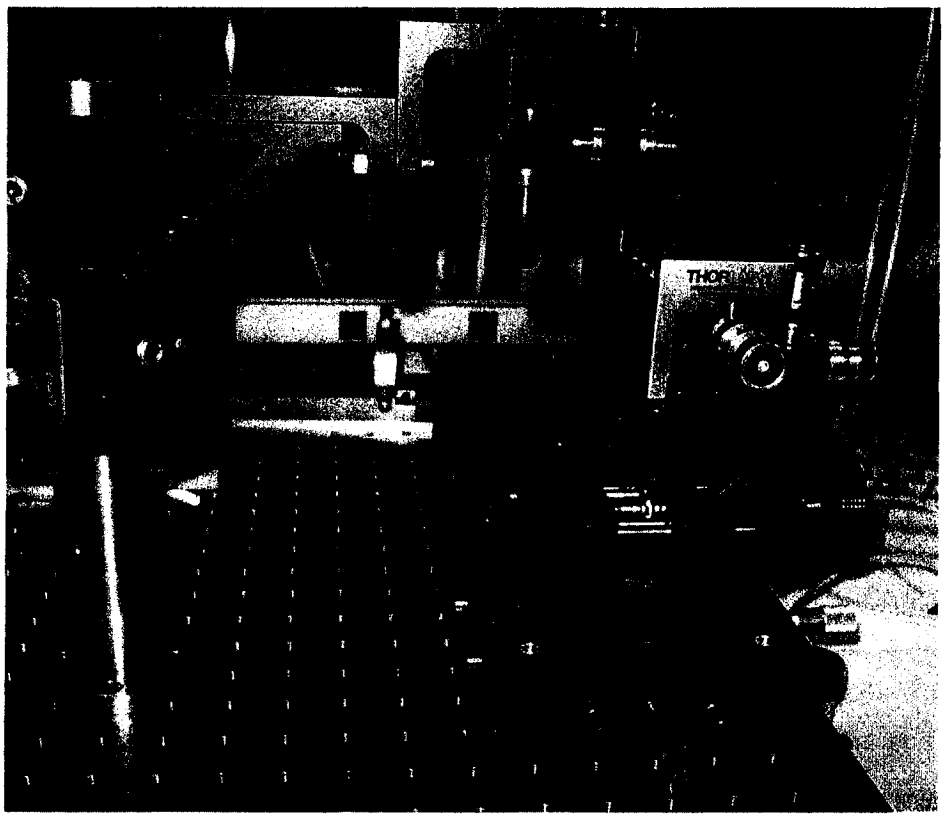

Figure 5.3 Coupling work stages for side-polished couplers

In order to couple two samples with polished fibers well, more dimensions should be considered to adjust the two parallel planes. In figure 5.4, it is a pitching adjustor and rotator, which can make tiny up and down adjustment in one side of the bottom plane. The other handgrip is used as controller of rotation adjustment. In figure 5.5, coarse and fine XYZ stages used to make fine three-dimension adjustor are shown.

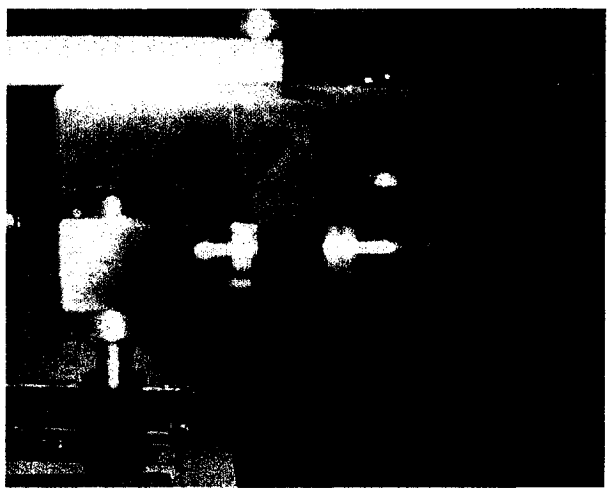

Figure 5.4 pitching adjustor and rotator

Figure 5.5 coarse and fine XYZ stages

5.1.2 Coupling experiment for the coupler with FBG

As shows in figure 5.6, a broad band Laser is used as a source of light, and it launched into a circulator port 1 that connected with the coupler at port 2. An OSA was connected with the circulator port 3 or with the output fibers of the coupler. It detected the reflection or the transmission of the coupler. If the OSA were connected with the other two output fibers of the coupler, it would detect the transmission light and coupling light (figure 5.6).

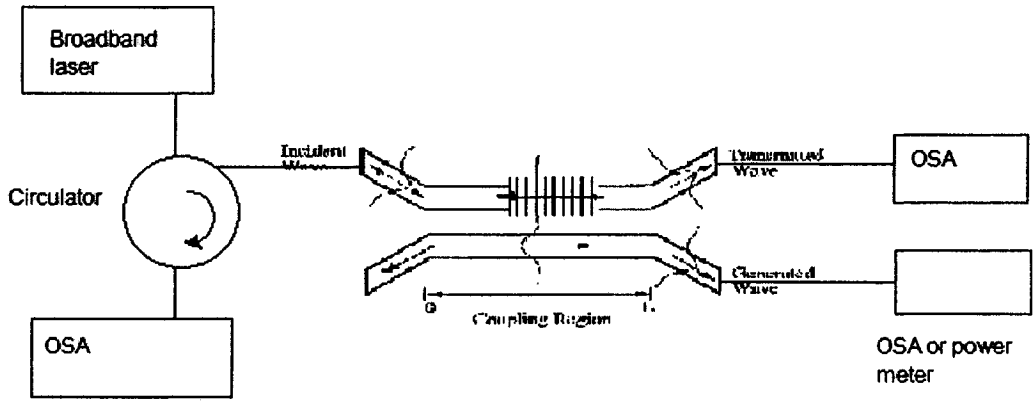

Figure 5.6 FBG fiber coupler testing set up

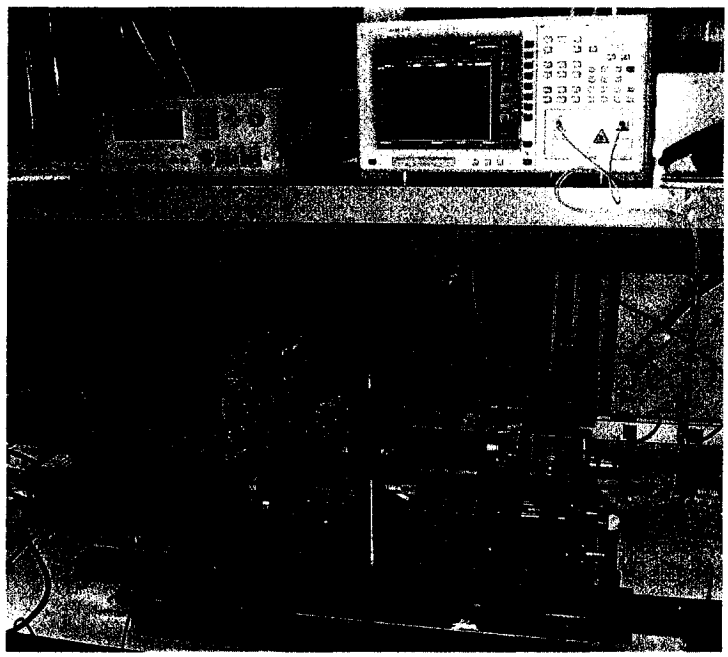

Figure 5.8 Tunable Laser and OSA involved in FBG fiber coupler testing

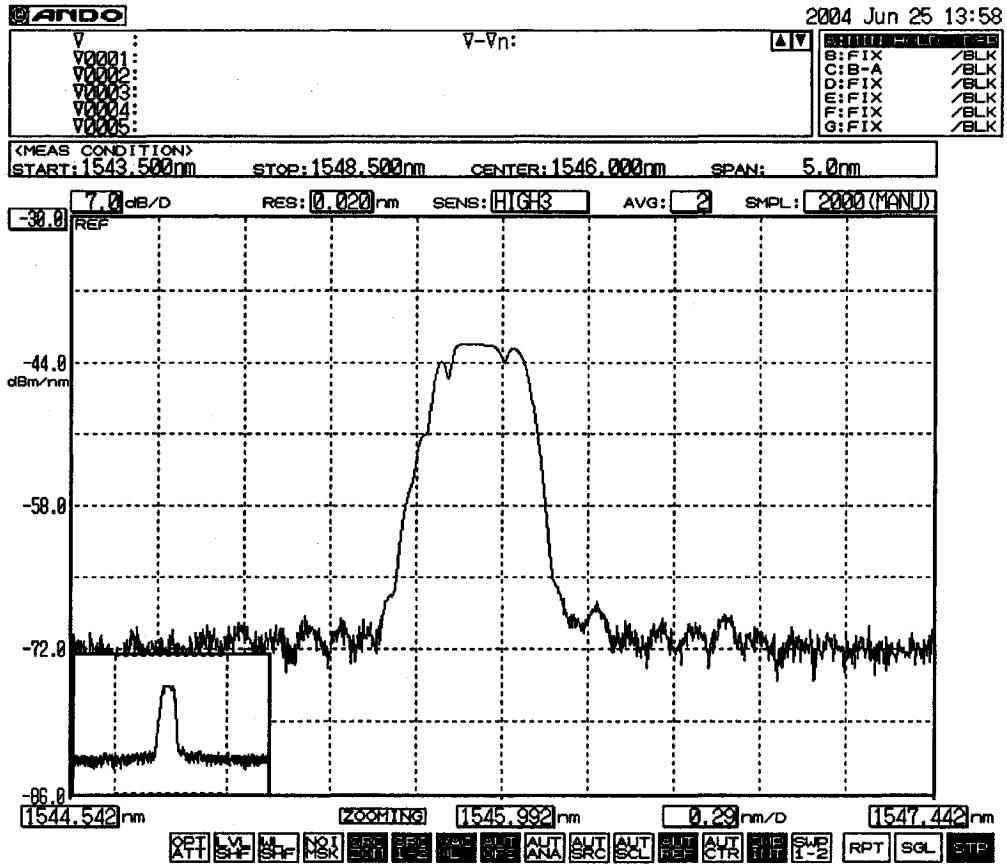

Figure 5.9 FBG fiber coupler reflectivity in OSA

5.2 Coupling Experiments

5.2.1 Laser light launched into and scattered from samples

Red light with $\lambda = 632.8nm$ was focused by a lens and launched into a SM side-polished fiber of a coupler. As shows in figure 5.10 and 5.11, red light was leaked out from side-polished. The scattered light at the coupling area also came out from a star coupler as it is shows in figure 5.12. Figure 5.13 shows scattered light in the sample of side-polished fibers on a glass substrate.

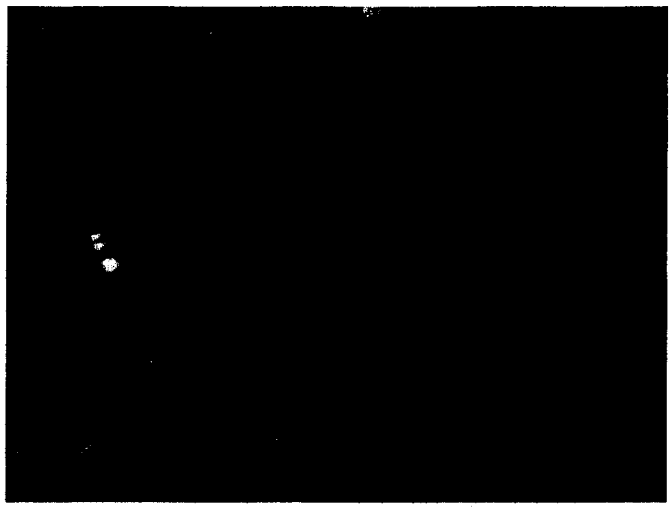

Figure 5.10 red laser light launched into the fiber and leaked from the sample

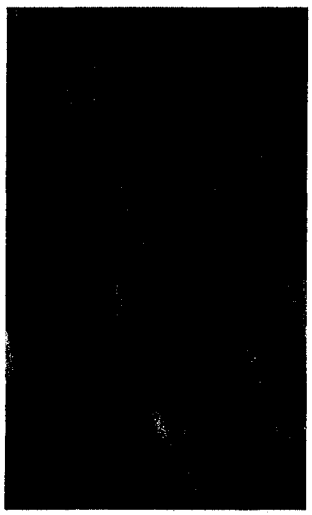

Figure 5.11 leaked light from the sample under microscope

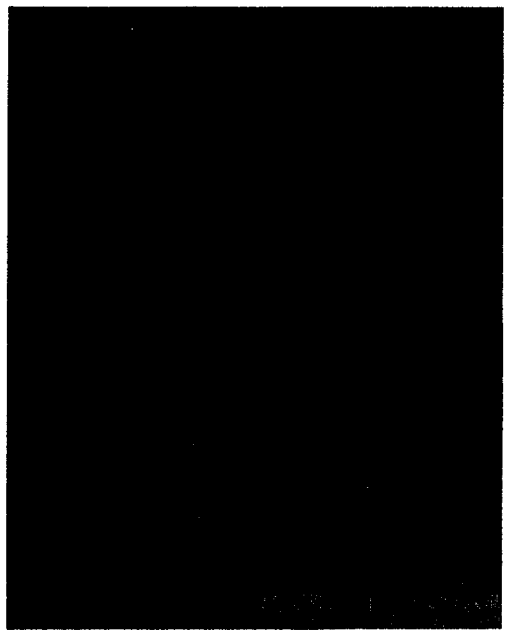

Figure 5.12 Laser launched into the fiber and scattered at the coupling area

Figure5.13 Fibers on a glass substrate light scattering

5.2.2 Light coupling in a star coupler

The star coupler we used is showed in figure 5.14 and 5.15. Optical fiber A, B, C, and D are all side-polished, and they are put close together with glue inter-media. The laser light was launched into the fiber A, and it could be coupled into fibers B, C or D when fiber A was moved to specific position.

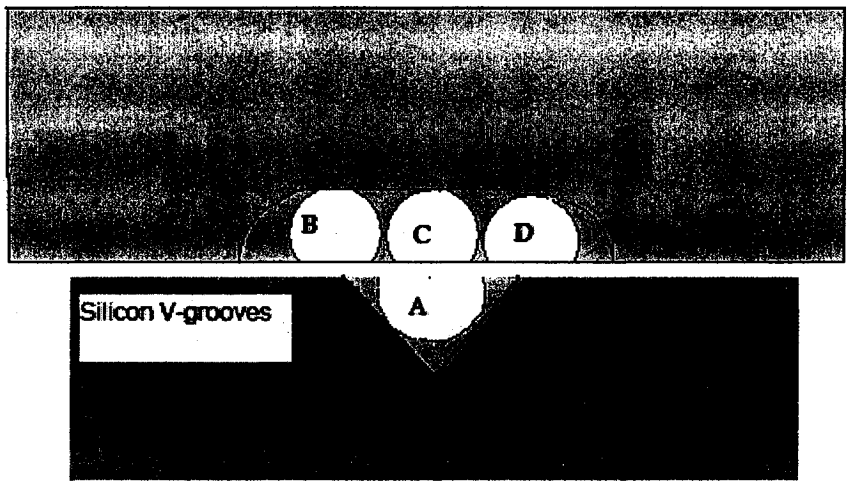

Figure 5.14 a star coupler model

Figure 5.15 a star side-polished coupler sample

Before putting silicon glue and bring them close enough, there was no light came out from the two fibers B and C, which is showed in a amplificatory picture. After moving the sample with fiber A close to another sample which has fiber B, C, and D on it,

the light was shining at fiber B in figure 5.15, 5.16. When the two sample move to a specific position, the input light are allowed coupling into Fiber B and Fiber C (see figure 5.17, 5.18 and 5.19)

Figure 5.15 one of the other fibers that shows light at the terminal section

Figure 5.16 background of the two fibers coupling

Figure 5.17 two of the other fibers that show light at their section

Figure 5.18 the amplificatory picture of the three fibers that show light at their section

Figure 5.19 background of the three fibers coupling

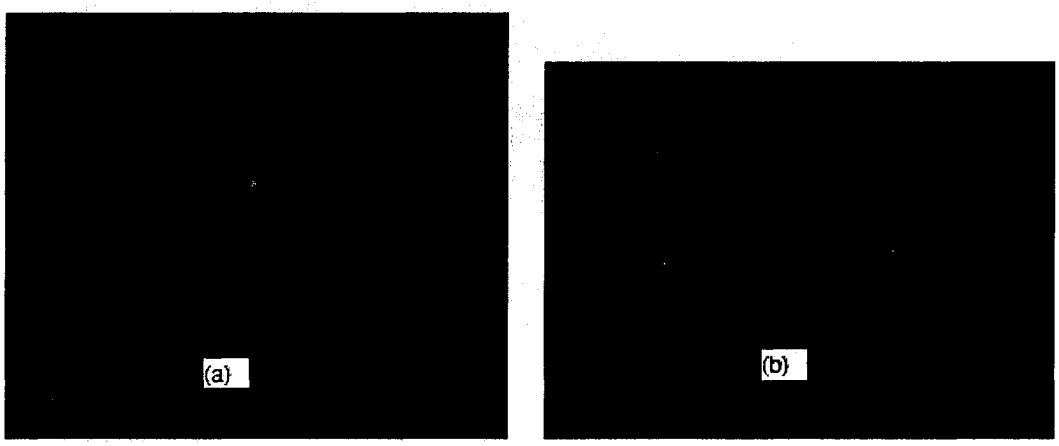

Figure 5.20 light intensity varied during these samples were adjusted

Figure 5.21, 5.22 and 5.23 are another set of pictures that indicated the light power variation among fibers of another star coupler when these samples were adjusted.

Figure 5.21 ligh from original coupling fiber A

Figure 5.22 light coupled into another fiber B

Figure 5.23 light coupled into three other fibers A, B, C

5.3 Application

As discussed in Chapter 4, V-grooves and side-polished fiber couplers are widely used in passive optical network, optical research, and sensor or MEMS area. In practice, it is necessary to launch laser light into MEMS devices on chips, and side-polished fibers can be used in these proposes. For example, when micro optical components were fabricated on Silicon wafer, V-grooves and side-polished fibers should be fabricated in lab in order to get successful experiment results. In sensing applications, side-polished SM fibers that combined with planar waveguide (PWG) or polyvinyl alcohol (PVA) based films work as UV sensors [1], temperature sensors [2], pH sensors [31], water detection sensors [32], and pressure sensors [33]. In optical network applications, by using their mechanical stability and low insertion loss, side-polished fibers and couplers

can be used as low loss laser couplers and amplifier launching couplers [34], tunable wavelength filters [35], modulators [36], switches [37], and amplifiers [38]. In dense wavelength-division-multiplexing (DWDM) systems, side-polished fiber couplers with fiber Bragg Gratings can work as Add-Drop-Multiplexers (ADM) [15], splitters, filters, interferometers etc.

Etched V-grooves are used to launch laser light into optical MEMS chips in MEMS experiments (figure 5.24). In optical communications, a polished fiber coupler with one or more FBGs could work as a splitter/filter or adder/dropper in specific wavelength.

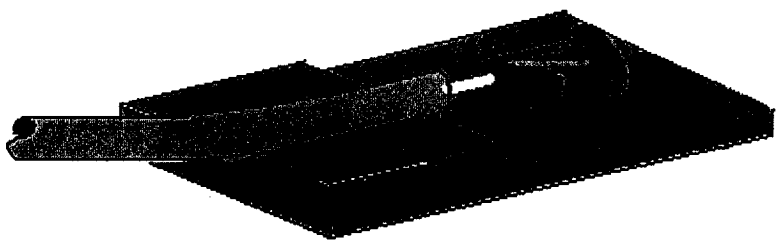

Figure 5.24 light launched to MEMS devices

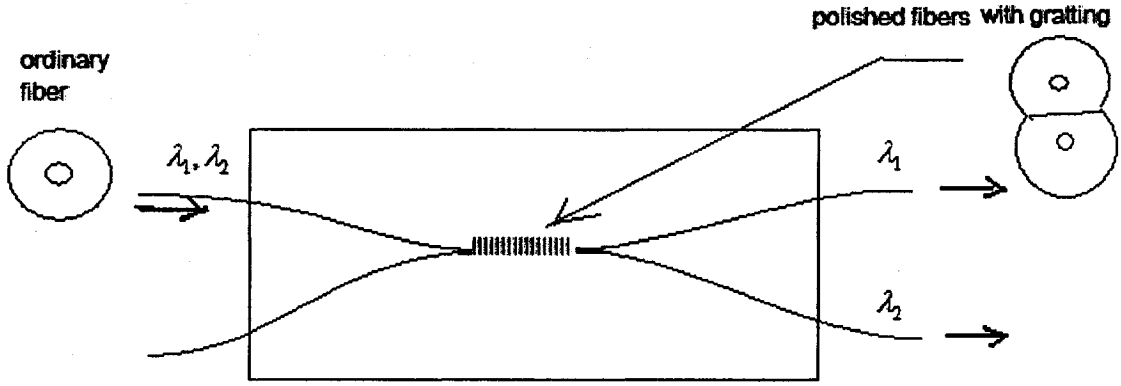

Figure 5.25 Side-polished fiber-types WDM with FBG

Figure 5.26 Side-polished FBG fiber-types WDM with two FBGs

If the gratings on fibers are slantwise chirped long period gratings, the device should become more complicated and have special profiles and applications. They could work as wideband adder/droppers, wideband splitter/filters and wideband switchers. By the way, the proposes of using slantwise long period grating is getting as much as possible light from core to cladding and transfer along the transfer direction of fiber signals. Figure 5.27 is the sketch map of a chirped Grating coupler that has wideband reflection characteristics

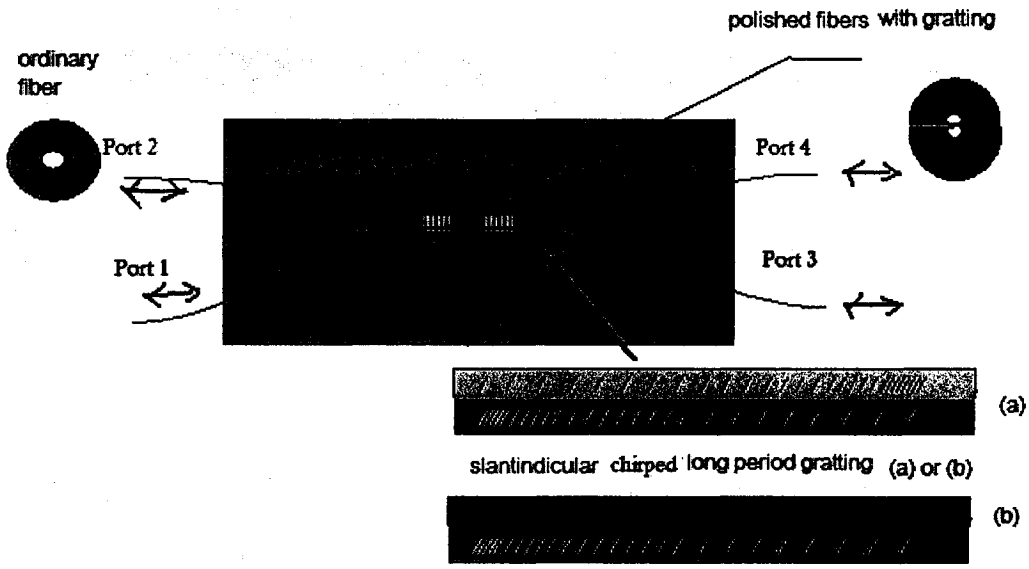

Figure 5.27 A side-polished slantwise chirped long FBG fiber device

The movement between the two faces of couplers could be detected and modulated in optical wavelength movement or coupling light power changing (figure 5.28). Figure 5.29 is the sketch of a single side-polished fiber detector or sensor.

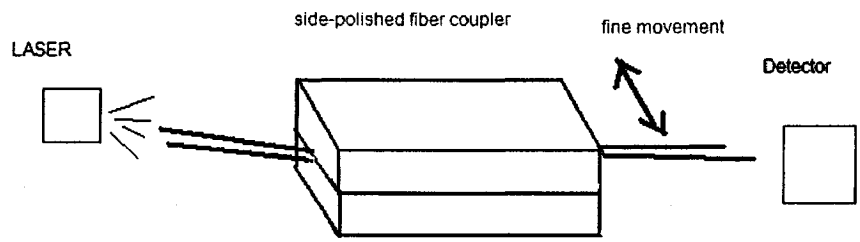

Figure 5.28 Side-polished fiber-types Movement modulator

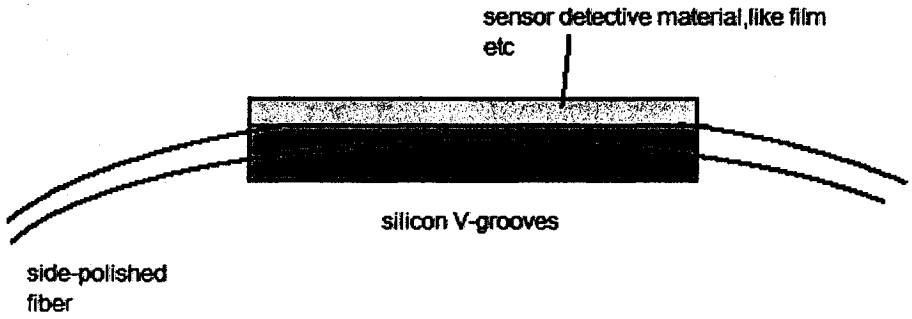

Figure 5.29 Side-polished fiber types sensor

Multi-fibers splices are only installed on ribbon type fiber optic cables. Multi-fiber splicing techniques can use arc fusion to restore connection, but most splicing techniques use mechanical splicing methods. The most common mechanical splice is the ribbon splice. A ribbon splice uses an etched silicon chip, or grooved substrate, to splice the multiple fibers within a flat ribbon (figure 5.32).

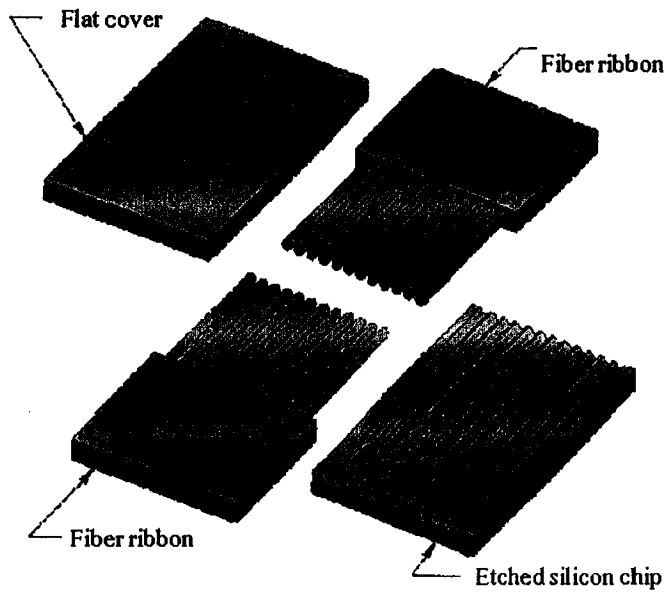

Figure 5.30 Ribbon splice on etched silicon chip.

CHAPTER 6

CONCLUSIONS AND SUGGESTIONS FOR FUTURE WORKS

6.1 Conclusion

The side-polished coupler is one of the most useful passive optical components in all-optical networks and integrates optical components. By using well designed Silicon V-grooves, expected side-polished fibers could be fabricated. Side-polished fibers and side-polished fiber couplers have wide applications in optical integrated components, MEMS, sensors, and all optic networks. 2x2 etched and star side-polished fiber couplers are well designed and fabricated in this work, and they are confirmed by experiments using a laser light with $\lambda = 632.8nm$.

Fiber transmission and couplers are simulated, and some conclusions, regarding the mode numbers and mode field diameter (MFD) with variation of the core and the cladding of the fibers are deduced as follow:

First of all, when the diameter of fiber core is reduced under 12μm, LP (1,1) was disappeared in the transmission of light. Secondly, the MFD of LP (0,1) mode is increased as the diameter of the fiber core was decreases. Thirdly, when the diameter of cladding is decreased, the MFD of LP(0,1) increased and it was found to be very dependent on the light wavelength. Furthermore, in lossless fiber couplers, the coupled power is distributed as a sine function of z, the coupler length, and the coupling coefficient is varying with the distance between the two fiber cores. Therefore, to make a SM fiber coupler, it is easy to get high coupling coefficient if a smaller core fiber is used and the two fiber core are placed closer to each other.

Etching fiber and side-polishing fiber are two of the methods to make fiber couplers at room temperature. Since etched fibers are so weak to be handled to make couplers without damages. Comparing with etched fibers, side-polished fibers are easier to be handled in fiber coupling processes, however, the etched fibers are very brittle and are very difficult to hand them. This is one of the disadvantages of these techniques.

An etched fiber with well-etched ditch and side etched fibers are fabricated, and imaginary models are discussed as good attempts since they are strong enough to be handled in coupling processes.

6.2 suggestions for future works

The coupler characteristics of coupled power, polarization, and dispersion need to be measured and quantitative analyzed.

In this work a kind of ditch based on Silicon P <110> wafer is designed as a suitable tool for coupling etched fibers. It needs to be fabricated and confirmed in making couplers. In addition, surface fiber etching, side-polished fiber etching and side-etched fiber technology are also need to be developed in the future to get different profiles.

Reference list

[1] Jong-Kuk Yoon, Gyoo-Won Seo, Kang-Min Cho, Kims, Sin-Won Kang : Controllable In-Line UV Sensor Using a Side-polished Fiber Coupler Coupler with Photofunctional polymer, IEEE photonics Technology Letters Vol 15, No 6, June, 2003

[2]. Alberto Alvarez-Herrero, H. Guerrero, T. Belenguer, and D. Levy: High-Sensitivity Temperature Sensor Based on Overlay on Side-polished Fibers. IEEE photonics Technology Letters, Vol 12, No 8, August, 2000

[3]. Mestdagh, Denis J.G.: Fundamental of Multiaccess Optical Fiber Networks. Artech House, pp. 20-26, 1995.

[4] J.H. Franz and V.K.Jain : Optical Communications Components and systems, Narosa Publishing House, pp 110-165, 2000.

[5] J. Parry-Hill and Michael W. : Davidson Thomas Young's Double Slit Experiment Matthew - National High Magnetic Field Laboratory, 1999

[6] Y. Wang, D.H. Park, and K.F. Brennan," Theoretical analysis of confined quantum state GaAs/AlGaAs solid-state photomultipliers," IEEE J. Quantum Electron, Vol 23, PP 76-84, 2000

[7]. Gerd Keiser: Optical Fiber communications Third edition, Mc Graw Hill, pp 50-65, 1999.

[8]. S.O. Kasap : Optoelectronics and photonics principles and practices, Prentice Hall, pp 145-155, 1998

[9] C.Pollock, "Fundamentals of Optoelectronics," Irwin, Chicago, pp 100-120, 1995.

[10] Donald,G. Baker: Monomode fiber optical Design. Van Nostrand Reinhold, New York, pp 134-154, 1987.

[11] Senior, J. M.: Optical Fiber communication-Principles and Practice. Second Edition, Prentice-Hall, 1992

[12] Green, Paul.E.Jr.: Fiber optical networks. Prentice-Hall, pp 115-150, 1993

[13] Pochi Yeh, Optical waves in layered media, John Wiley & Sons, inc(1988)

[14]. A yaruv and P. Yeh, Optical Waves in Crystals, John Wiley & Sons, inc(1984)

[15] I. Baumann, J. Seifert, W. Nowak, and M. Sauer, " Compact all fiber add-drop-multiplexer using Fiber Bragg Gratings," IEEE photonics Lett., vol., no. 10, Oct., 1996

[16] Hui Zhang : Analysis and fabrication of grating assisted optical components, thesis of Master degree of Concordia University, pp 30-55, 1994.

[17]. ZHONG-MING MAO, XI-SHENG FANG, AND BIN-HONG LI " Mode Excitation Theory and Experiment of Single-Mode Fiber Directional Coupler with Strong Coupling" JOURNAL OF LIGHTWAVE TECHNOLOGY, VOL. LT-4, NO. 4, APRIL 1986

[18] A. W. Snyder, "Coupled-mode theory for optical fibers," J. Opt. Soc. Amer., vol. 62, pp. 1267-1277, 1972.

[19] F. Sporleder, and H.-G. Unger. Waveguide Tapers Transitions and Couplers. London, England: Peter Peregrinus, pp 100-120, 1979.

[20] L. Eyges, and P. Wintersteiner, "Modes of an array of dielectric waveguides," J. Opt. SOC. Amer., vol. 71, pp. 1351-1360, 1981.

I21] A. W. Snyder, "Polarising beam splitter from fused taper couplers," Electron. Lett., vol. 21, pp. 623-625, 1985.

[21] O.Than, S.Buttgenbach, "Simulation of Anisotropic Chemical Etching of Crystalline ilicon Using a Cellular Automata Model, " Sensor and Actuator A, Vol 45, pp. 85-89, 1998

[22] Landsberger "Micotransducer Process Technology" ELEC-6251 text book , part II pp. 100- 250, 2002

[23] "Semiconductor technology handbook " Technology associates copyright Feb. pp 58-65, 1993.

[24]. S.Wolf and R. Tauber, "Silicon Processing:Vol.1", Lattice Press, CA, 1986

[25] R. T. Howe and R.S. Muller, "stress in polycrystalline and amorphous silicon micromechanical beams," J. Appl. Pys. Vol 54 . pp 4674-4675, 1998

[26] H. Guckel, T. Randazzo, and D.W. Burns, "A simple technique for the determination of mechanical properties," Sensors Actuators. Vol. 4. pp. 447-454, 1983.

[27]. R. T. Howe, " Polysilicon integrated microsystems: Technology and applications," in Proc. 8th int. conf. Solid-state Sensors Actuators, Stockholm, Sweden, June 25-29, pp.43-46. 1995.

[28] Jun Chen, " Characterization of Material Surface by using Fiber Bragg Grating", Thesis of Master degree of Concordia University, 2005

[29] Biswanath, Mukherjee " Optical Communication Networks", Mcgraw-Hill, pp 111-118, 1999.

[30] R. Hull "Properties of Crystalline Silicon " INSPEC, London, pp 150-168, 1999.

[31] D. Flannery, S.W. James, R.P. Tatam, and G.J.Ashwell, "PH sensors using Langmuir-Blodgett overlays on polished optical fibers," Opt. Lett., vol. 15, no.8, pp 567-569,1997.

[32] K.R. Sohn, K.T. Kim, and J.W. Song, " Optical fiber sensor for water detection using a side-polished fiber coupler with a planar glass-overlay-waveguide," Sens. Actuators A, vol. 101, pp.137-142,2002.

[33] J.K. Yoon, S.W. Kim, G.W.Seo, Y.S.Yu, D. H. Kwon, and S.W. Kang,"Side-polished fiber optical pressure sensor based on stress optical property of polymer planar waveguides," Sens, Materials, vol. 14, no. 4, pp. 219-230, 2002.

[34] E. Mao, C.- C. Lin, O. Solgaard, and J. S. Harris, Jr. D. R. Yankelevich and A. Knoesen, " Narrow-band light emission in a semiconductor-fiber asymmetric waveguide coupler," IEEE 2000

[35] W. Johnstone, G. Brierley, D. moodie, R. Varshney, and B. Culshaw, " fiber optic wavelength channel selector with high resolution," Electron, Lett., vol. 28, pp. 1364-1365, 1992.

[36] W. Johnstone, S. Murray, G. Thrusby, M. Gill, A. McDonach, D. Miidie, and B. Culshow, " Fiber optical ,odulators using active multimode-waveguide overlays," Electron, Lett., vol. 27, pp 894-896, 1991.

[37] K. McCallion, W. Johnstone, and G. Thrusby, " Investigation of optical fiber switch using a electro-optic interlays," Electron, Lett., vol. 28, pp 410-411, 1992.

[38] A. Gloag, N. Langford, K. MaCalllion, and W. Johnstone, " unable erbium fiber laser using a novel overlay bandpass," Opt, Lett., vol. 19, pp 801-803, 1994.

[39] I. Baumann, J. Seifert, W. Nowak, and M. Sauer, " Compact all fiber add-drop-multiplexer using Fiber Bragg Gratings," IEEE photonics Lett., vol., no. 10, Oct., 1996.

[40] A. Ankiewicz, A. W. Snyder and X. –H. Zheng, " Coupling between parallel optical fiber cores – critical examination," J. lightwave Tech. vol. 4, pp. 1317-1323. Sept. 1986.

[41] A. Takagi , K Jinguji, and M. Kawachi, " Wavelength characteristics of 2x2 optical channel-type directional couplers with symmetric or nonsymmetric coupling structures," J. Lightwave Tech. vol. 10. pp. 735-746, June 1992